Diode Laser-Pumped Solid-State Lasers

TSO YEE FAN AND ROBERT L. BYER, FELLOW, IEEE

Abstract—**Recently, interest in diode laser-pumped solid-state lasers has increased due to their advantages over flashlamp-pumped solid-state lasers. We present a historical overview of semiconductor diode-pumped solid-state lasers beginning with work in the early 1960's and extending to recent work on wavelength extension of these devices by laser operation on new transitions. Modeling of these devices by rate equations to obtain expressions for threshold, slope efficiency, and figures of merit is also given.**

I. Introduction

THERE has been a recent surge of interest in the use of semiconductor diode lasers as pump sources for solid-state lasers. With diode laser pumping, it is possible to build higher efficiency and therefore simpler and more compact lasers in an all solid-state device. These advantages were recognized in the early days of lasers [1], [2], but until recently, the performance of diode lasers was inadequate in terms of reliability, ease of handling, operational lifetime, and output power to be employed as practical pump sources. With recent progress in the development of reliable higher power diode lasers, parallel improvements in diode-pumped solid-state lasers have occurred. Diode laser-pumped solid-state lasers also offer advantages over the direct use of diode lasers themselves. These advantages include narrower frequency linewidth, better beam quality, higher peak powers, and different wavelengths.

Our group at Stanford has studied diode laser-pumped solid-state lasers for the past few years. Our efforts have been concentrated in the areas of frequency stable devices, single-longitudinal mode lasers, different Nd^{3+} doped host materials from Nd:YAG, wavelength diversity through harmonic conversion, and new transitions in rare earth ions. This paper presents an overview of a number of aspects of these devices. We begin with a historical review of the field. It has not been widely recognized that the history of diode laser-pumped solid-state lasers extends to the early 1960's. The overview is followed by a discussion of rate equation models to describe continuous-wave (CW) end-pumped devices and derive scaling laws and figure of merits. Finally, the possibility of operating new transitions in trivalent rare earth ions is presented as a way of extending the output of these devices to new wavelengths.

Manuscript received December 16, 1987; revised February 1, 1988. This work was supported by the U.S. Army Research Office, the Air Force Office of Scientific Research, and NASA.

T. Y. Fan was with the Edward L. Ginzton Laboratory, Stanford University, Stanford, CA 94305. He is now with M. I. T. Lincoln Laboratory, Lexington, MA 02173.

R. L. Byer is with the Edward L. Ginzton Laboratory, Stanford University, Stanford, CA 94305.

IEEE Log Number 8820788.

II. Historical Overview

The initial ideas and demonstration of the use of semiconductor diode lasers and light emitting diodes (LED's) as pump sources for solid-state lasers date back to the early 1960's. The first section of this historical overview covers this early work. This is followed by sections on the use of Nd:YAG and stoichiometric Nd compounds as gain media. Then guided wave structures and other devices to allow different wavelengths and higher peak powers are covered followed by a review of recent work.

A. Early Work

The first mention of the use of semiconductor sources to pump a solid-state laser to our knowledge was by Newman [1] who found that radiation near 880 nm from recombination in GaAs diodes, essentially an LED, could excite fluorescence near 1.06 μm in $Nd:CaWO_4$. He states

> "The small size and simple structure of the diodes will make possible a direct coupling of the pumping radiation to the laser without any complex optics. This in turn will greatly reduce the size and cost of the functional devices. The efficiency of conversion of input pump power to output power, both as regards the pump source and the internal conversion of energy within the laser, may permit continuous power output several orders of magnitude higher than is presently possible."

While some of the claims are optimistic, it is clear that some of the potential advantages of semiconductor sources over lamps were understood even at this early stage of laser development. The energy level diagram of the Nd^{3+} ion and the transitions used in this experiment are shown in Fig. 1 with the pump transition and proposed laser transition indicated.

Next, Keyes and Quist [2] demonstrated the first diode laser-pumped solid-state laser shortly after the development of the first GaAs diode lasers [3]–[6]. The solid-state laser was $CaF_2:U^{3+}$ at 2.613 μm. A schematic of the laser is shown in Fig. 2, and the energy level scheme is shown in Fig. 3(a). The five diode lasers were arranged in a side pumping or transverse geometry in which the pump radiation is incident on the gain medium in a direction perpendicular to the resonator axis. An additional integrating chamber was placed around the assembly to try

0018-9197/88/0600-0895$01.00

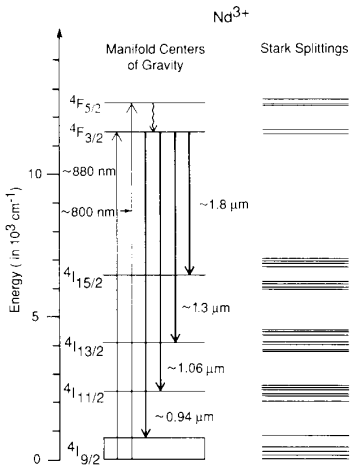

Fig. 1. Energy level diagram of Nd^{3+}. The laser transitions are shown in heavy lines, diode pump transitions in light lines, and relaxation in wavy lines. The first proposed diode-pumped laser transition was ${}^4F_{3/2}$–${}^4I_{11/2}$ near 1.06 μm pumped at 880 nm. Representative Stark splittings of the manifolds are shown on the right-hand side. The actual laser transitions occur between these individual Stark splittings. The open box for the ground-state manifold indicates that the laser transition to this manifold is to an energy level above the ground state.

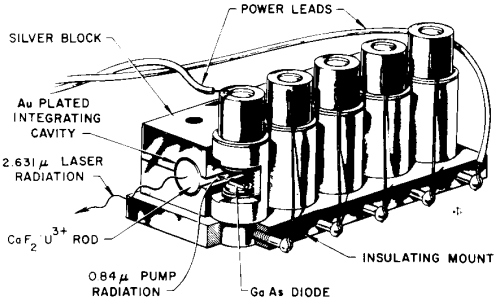

Fig. 2. Schematic of the first diode-laser pumped solid-state laser U^{3+} : CaF_2 from [2]. The diodes are arranged for pumping in a transverse geometry.

to capture all of the pump radiation. The entire assembly was placed in a liquid helium dewar because the early diode lasers needed to be cooled to obtain operation, and the lower laser level in $CaF_2 : U^{3+}$ is 609 cm^{-1} above the ground state. The lower laser level population is given by the Boltzmann distribution; cooling reduces this population and therefore the threshold. Quasi-CW operation with emitted pulses longer than one upper state lifetime was obtained with thresholds near 3 W of incident power on the laser rod over 500 μs. Keyes and Quist also recognized the advantages of diode laser pumping over flashlamps. They noted that the use of GaAs diode lasers should be ideal for pumping of Nd^{3+} lasers and that such devices should be more efficient than lamp pumping. This would induce less heating in the gain medium and reduce the thermal problems of high-energy lasers.

A third example of early work is that of Ochs and Pankove [7] who used arrays of LED's to pump a $CaF_2 : Dy^{2+}$ laser. The energy level scheme is shown in Fig. 3(b). The

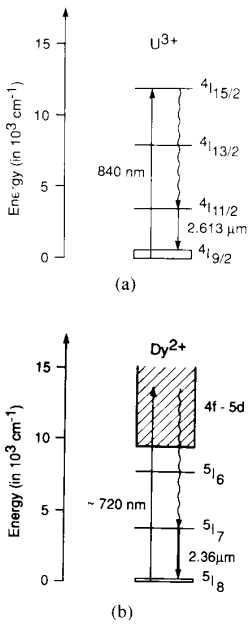

Fig. 3. Energy level schemes in early diode-pumped lasers. (a) U^{3+}. (b) Dy^{2+}.

pump wavelength is ~720 nm, and laser action is at 2.36 μm to an energy level 29 cm^{-1} above the ground state. A transverse pump geometry was used with ten LED arrays with ten LED's in each array arranged cylindrically around a laser rod. The LED's and laser rod were cooled to 1.9 K for good LED performance and reduction of the lower laser level population in Dy^{2+}. Quasi-CW operation was obtained with thresholds about 0.1 W incident on the laser rod. After these early works, interest shifted to Nd : YAG because the Nd^{3+} ion offers excellent spectroscopic properties for diode-pumped solid-state lasers.

B. The Shift of Interest to Semiconductor-Pumped Nd : YAG Lasers

The Nd^{3+} is an excellent dopant for semiconductor-pumped solid-state lasers. There is strong absorption in the emission bands of GaAs, GaAlAs, and GaAsP LED's and diode lasers. The absorption spectra of two Nd^{3+} doped materials near 800 nm, Nd : YAG and Nd-doped phosphate glass are shown in Fig. 4. Ions excited into the pump bands relax efficiently to the upper laser level. From this upper laser level, there are two four-level transitions with high gain, the ${}^4F_{3/2}$–${}^4I_{11/2}$ and ${}^4F_{3/2}$–${}^4I_{13/2}$; thus, laser action can easily be achieved with low thresholds. As shown in Fig. 1, each of the ${}^{2S+1}L_J$ manifolds is split by the crystal field into $J + 1/2$ doubly degenerate energy levels. The positions of these levels are different for each host, although the centers of gravity of each manifold are approximately the same. The relative desirability of a material as a gain medium is dependent on not only its spectroscopic properties, but other aspects such as thermo-mechanical properties and ease of crystal growth. By the early 1970's YAG had become the Nd^{3+} doped

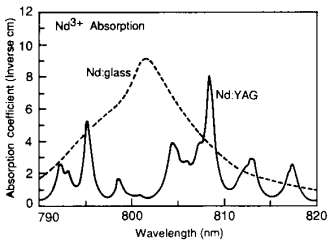

Fig. 4. Absorption spectrum in 1.1 percent doped Nd : YAG and 3 percent doped Nd : glass around 800 nm.

host of choice for lamp pumping due to its superior combination of spectroscopic, thermomechanical, and growth properties.

Ross [8] demonstrated the first diode laser-pumped Nd : YAG laser. This was pumped by a single GaAs diode laser in a transverse geometry. The YAG rod was at room temperature, but the diode laser was at 170 K to shift its wavelength to the absorption band in Nd : YAG at 867 nm. Ross recognized that the use of diodes as pump sources for solid-state lasers offered advantages over direct use of diodes. He noted that solid-state lasers can act as temporary energy storage devices due to their long upper state lifetime. This allows the output of many diode lasers to be collected in the gain medium and the energy released in a short pulse to achieve high peak powers. He also noted that the output of solid-state lasers could have a much narrower solid angle so brightness can be enhanced and that the spectral bandwidth of the solid-state laser is narrower than that of diode lasers. While diode laser technology has improved substantially since Ross's paper, these advantages still exist.

There followed a number of reports on transverse geometry, LED, and diode laser-pumped Nd : YAG lasers. Near room temperature [9], [10] and room temperature [11], [12] CW operation pumped by arrays of $GaAs_{1-x}P_x$ LED's was shown. Barnes [13] made the first attempt to model these LED, side-pumped Nd : YAG lasers. Approximate expressions for threshold and slope efficiency were derived.

Conant and Reno [14] also demonstrated a side-pumped device with diode laser pumping. They recognized that diode lasers have higher brightness than LED's and therefore the pump radiation could be absorbed in a smaller volume which should lead to lower threshold due to higher gains. Both the Nd : YAG laser rod and GaAs diode lasers were cooled, and about 6 percent optical-to-optical efficiency was achieved for a rod temperature of 250 K. The work was limited to the pulsed mode because of the limitations of the diode lasers. The average output power as a function of absorbed pump power is shown in Fig. 5. Threshold was 0.56 W with slope efficiency of 16 percent. Up to 120 mW of output power for 1.3 W of absorbed power was obtained. Jackson and Rice [15] also side pumped with diode lasers. They studied the use of bursts of short pulses to drive the Nd : YAG laser in a quasi-CW mode. The bursts were longer than the upper

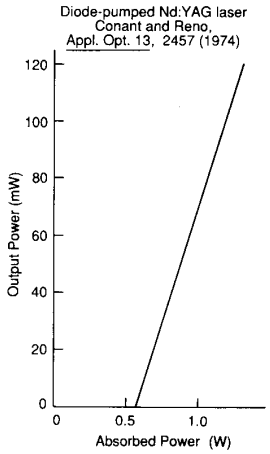

Fig. 5. Average output power as a function of average absorbed pump power in a transverse-pumped Nd : YAG laser reported in [14].

state lifetime and consisted of pulses with a repetition rate of 100's of kHz. The use of bursts of short pulses was necessary since diode lasers at this time could not be run true CW. They found that the pulse repetition rate must be on the order of 1 MHz to achieve quasi-CW laser operation with low ripple on the Nd : YAG laser output.

Farmer and Kiang [16] did an extensive study of transverse geometry LED-pumped Nd : YAG lasers. They explored issues such as coupling of the LED radiation to the laser rod, fabrication and output spectrum of GaAlAs LED's, and rate equation analyses to derive the output power and find the effects of pump modulation. They obtained significant improvement in efficiency by use of an index matching technique to couple the pump radiation to the laser rod. However, they noted that the laser gains in such LED-pumped Nd : YAG lasers were too small for the insertion loss of additional cavity elements such as mode lockers or frequency-doubling crystals to be tolerated.

Work on LED-pumped Nd : YAG lasers in the transverse geometry was also performed in the Soviet Union [17]–[21]. While the output power in initial experiments was poor since the operating point was barely above threshold [17], [18], later quasi-CW output powers of 1 W were demonstrated [19] which was the best reported at the time from LED-pumped systems. Bilak *et al.* [20] studied different geometries for placing the LED arrays around the gain element. They were also able to demonstrate laser action on the 1.32 μm transition as well as the 1.06 μm transition in Nd : YAG. In addition, an LED-pumped ring laser was developed for use as a rotation sensor [21]. LED pumping allowed more stable operation of the device because of the need for less cooling compared to a lamp pumped system.

In parallel to this work on side-pumped geometries, there was also investigation into the end-pumped geometry which offers the advantage that the pump light can be efficiently coupled into the laser mode, but has the disadvantage of limiting the number of diode lasers or LED's. Rosenkrantz [22] demonstrated the first reported pulsed,

diode laser-pumped device in an end-pumped geometry. He recognized that this geometry offers the advantage of more efficient absorption of pump radiation compared to the transverse geometry because the pump radiation is collinear with the laser mode. Thus, longer absorption paths are possible with a large fraction of the pump power within the laser mode volume. Simple expressions are derived for threshold pump energy in a pulsed mode with rough agreement with experiment.

Other reports of end-pumped Nd : YAG lasers followed [23]–[28]. Nearly CW operation below room temperature was shown pumping with a single LED [23], [24]. Chesler and Singh [25] modeled this laser with the assumptions of uniform pumping and both multimode and single transverse mode extraction, and rough agreement between the observed and calculated thresholds was achieved. True CW operation at room temperature was demonstrated using superluminescent diodes (SLD) as pump sources [26], [27]. Ostermayer [28] showed that a single LED could be used to obtain end-pumped operation of a CW Nd : YAG laser at room temperature.

There has been other work in diode pumping Nd : YAG which is discussed in a later section. In the mid-1970's, a new class of solid-state laser materials were developed called stoichiometrics which have some favorable properties for diode pumping.

C. Stoichiometric Nd Lasers

One difficulty with Nd^{3+} doped materials is that the allowed concentration of Nd is limited due to concentration quenching of the upper state lifetime. However, it is often desirable to have high doping densities because the pump light can be absorbed in a small volume to achieve higher gains for the same pump power. A class of materials called stoichiometrics was discovered in which Nd^{3+} is no longer a dopant, but instead a chemical component of the crystal itself. These materials have less concentration quenching than Nd : YAG. Due to the high doping density, over an order of magnitude larger than that of Nd : YAG, efficient absorption of the pump light is possible in a small volume.

The first such laser was NdP_5O_{14}(NPP) [29] pumped by a pulsed dye laser. In the initial experiment, the laser threshold for an end-pumped NPP laser is significantly higher than for Nd : YAG, but the authors projected a lower threshold for NPP compared to Nd : YAG in a transverse-pumped geometry. They noted that NPP was a promising material for diode laser and LED pumping [29], [30]. While much of the research in stoichiometric Nd materials was aimed at eventually using semiconductor pumping, this review does not cover the whole field of stoichiometrics; for a more complete overview, there are two good review papers on this topic [31], [32].

Chinn *et al.* [33] used a rhodamine 6G (R6G) dye laser operating near 580 nm to transverse pump NPP. Experimental thresholds as low as 4 mW led to predicted threshold powers for LED pumping of 8.5 mW based on modeling of the device. A threshold power of 7 mW under diode laser pumping with an overall 7 percent optical-to-optical efficiency was subsequently demonstrated [34], [35]. Further work on side pumping of stoichiometrics was carried out by Saruwatari and Kimura [36] and Budin *et al.* [37], [38]. Both groups pumped with an LED array and were able to achieve below room temperature operation. Budin *et al.* [37] noted that they were limited in the pump power density due to the relatively low brightness of the LED's.

Lasers with an end-pumped geometry have also been studied in these materials. Saruwatari *et al.* [39] and Saruwatari and Kimura [36] demonstrated LED-pumped operation in $LiNdP_4O_{12}$ (LNP) at $-35°C$. Room temperature operation in this early work was not possible due to a slightly populated lower laser level at room temperature, but was later demonstrated using a higher power, higher brightness diode laser [40]. Good laser operation on both the 1.05 μm and the 1.32 μm transitions in LNP was achieved by Kubodera and Otsuka [41] by diode laser pumping. Output powers of 2 mW for 12 mW input power at 1.05 μm and 0.5 mW for 11 mW at 1.32 μm were demonstrated in single transverse and single longitudinal mode operation at room temperature. In a similar experiment, Zverev *et al.* [42] obtained 0.6 mW at 1.047 μm for 6 mW absorbed power in LNP. Phosphate glasses of essentially the same composition as the stoichiometrics were also used as gain elements [43]. These are attractive because they are simple to fabricate. Laser action was demonstrated under LED pumping in a pulsed mode.

D. Guided-Wave Devices

The use of guided wave structures instead of bulk devices is also of interest for diode pumping. One reason is the compatibility of guided wave devices with optical fiber systems. Another reason is that by guiding both the pump wave and the laser mode, higher pump densities and therefore gain compared to bulk devices can be achieved.

The first report of a guided wave device was by Stone and Burrus [44] who end pumped a multimode, Nd-doped, silica-based, glass fiber laser. The cavity was provided by either depositing reflector coatings directly onto the end of the fiber or by external mirrors. Typical core diameters were 35 μm with lengths of 1 cm. CW thresholds in these devices were less than 1 mW. This technique was extended to Nd : YAG fiber lasers [45]–[47]. These devices were 50–80 μm in diameter, 0.5 cm long and were end pumped with LED's. Laser operation on both the 1.06 μm and 1.3 μm transitions was demonstrated with output powers of up to 1 mW on the 1.06 μm transition.

Waveguiding structures were also considered for a transverse pump geometry [48]. Such a device may offer advantages such as small resonator construction and good transverse mode stability. Design calculations were performed for an LED array-pumped, rectangular cross section waveguide fabricated of a number of Nd laser materials including Nd : YAG, NPP, and LNP. Such a device

made of an LNP gain medium with a glass cladding was demonstrated using Ar^+ laser pumping [49], [50].

E. Other Devices

Most of this initial work in diode pumping concentrated on designing and demonstrating simple Nd-doped devices. However, there was also work reported on diode pumping of other ions, insertion of intracavity second harmonic generation (SHG) crystals, and driving of spiking oscillations, Q switching, and mode locking to achieve higher peak powers.

Laser action was demonstrated at 1.029 μm in a transverse geometry, Si-doped GaAs LED array pumped Yb:YAG laser [51]. The energy level diagram of this transition is shown in Fig. 6(a). Since the lower laser level is only 611 cm^{-1} above the ground state, the laser was cooled to 77 K. The Si doping of the LED's shifts the emission wavelength to provide a better spectral match to the Yb^{3+} absorption. A room temperature, LED-pumped $LiYbF_4$:Tm, Ho laser was proposed where the Yb^{3+} absorbs the pump radiation [52]. This excitation is transferred to Tm^{3+} and then to Ho^{3+} with the laser transition on the $^5I_7$–$^5I_8$ Ho^{3+} transition. The energy level scheme is shown in Fig. 6(b). The difficulty is again that the lower laser level is in the ground state manifold. This material was investigated spectroscopically, and lamp-pumped laser operation at 77 K was demonstrated, but no diode-pumped device was attempted.

Another way to achieve wavelength diversity is by frequency conversion. In the earliest diode-pumped devices, the gain was too low for the insertion of intracavity elements [16]. With improvement in semiconductor pump sources, such devices could be constructed. Chinn [53] demonstrated a longitudinal geometry, intracavity frequency-doubled NPP laser pumped by a dye laser. Thresholds of 5 mW and outputs of 1 mW single ended were achieved; the author notes that with simple optimization, semiconductor pumping of this source should be possible. Actual demonstration of such a device was made by Kuratev [54] who used a $BaNaNb_5O_{15}$ crystal to intracavity double an LED array pumped Nd:YAG laser.

Spiking oscillations, Q switching, and mode locking of semiconductor-pumped Nd^{3+} doped lasers have been considered for higher peak power operation. Spiking oscillations have been shown by modulation of the pump light [12], [35], [55]. Under deep modulation of an LED-pumped Nd:YAG laser, 100 times peak power enhancement over the CW output was obtained [12]. Both shallow [35] and deep [55] modulation were investigated in stoichiometric diode pumped lasers with peak power enhancements of 11 and 23, respectively.

Mode locking was investigated in stoichiometric lasers. Chinn and Zwicker [56] demonstrated a 14 ps pulse from an end-pumped FM mode-locked $Nd_{0.5}La_{0.5}P_5O_{14}$ excited by a CW rhodamine 6G dye laser. Otsuka *et al.* [57] demonstrated a similar device in LNP with 49 ps pulse with under Ar^+ laser pumping. Both groups note that semiconductor pumping of these systems is possible for miniaturization.

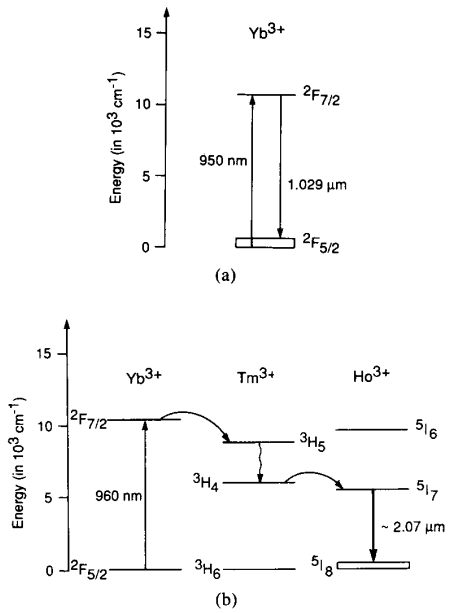

Fig. 6. Energy level schemes of diode-pumped solid-state lasers. (a) Yb^{3+}:YAG, (b) Tm, Ho:$LiYbF_4$. Arrows between ions indicate energy transfer.

Q switching was demonstrated in LED-pumped Nd:YAG and Nd-doped potassium–gadolinium tungstenate (PGT) [54]. A number of different techniques for Q switching were used including electrooptic, acoustooptic, saturable absorber, and cavity dumping. Pulse lengths as short as 4 ns using cavity dumping were obtained, with the highest peak power being 170 W in a 65 ns pulse in Nd:PGT by acoustooptic mode locking.

F. Recent Work

With improvements in diode laser technology in the early 1980's to allow higher powers and longer operational lifetimes, the interest in semiconductor pumping turned to using only diode lasers as pump sources. Progress was made in stoichiometrics, Nd:YAG systems, and guided wave devices.

Stoichiometrics were of interest for miniature lasers for communication systems at 1.3 μm. Kubodera and Noda [58] demonstrated a GaAlAs diode laser-pumped, single-axial mode LNP laser with up to 1.4 mW output. Seven laser diodes were used in an end-pumped geometry. Optical fibers were used to bring the output of the diode lasers to the LNP crystal and direct the power from these seven diodes to the same spot on the crystal. The device was used as a source for a transmitter of a fiber optic communication system. A tunable NPP source near 1.3 μm was investigated by Telle [59]. The laser was tuned with a grating over ~40 nm range with an Ar^+ laser excitation source in an end-pumped configuration. Under diode laser pumping, tuning was limited to a few nanometers because of the relatively low pump power.

Progress has also been made in end-pumped and side-pumped Nd:YAG systems. Longitudinal geometry, monolithic, diode laser-pumped Nd:YAG lasers have been shown to be frequency stable by Zhou *et al.* [60]. The frequency jitter of less than 10 kHz was over an order of magnitude better than that observed under lamp pumping. The efficiency, up to 1.5 percent overall electrical to optical, and compactness of the diode laser-pumped device allows operation without water cooling so the technical noise is reduced compared to a lamp-pumped device. A schematic of this device is shown in Fig. 7. Sipes [61] showed that the high efficiencies predicted for diode laser-pumped solid-state lasers could be realized in practice. An overall electrical to optical efficiency of 8 percent was shown in a diode laser array-pumped Nd:YAG laser in a longitudinal geometry. He projected, through simple scaling arguments, that output power of up to 1 W with efficiencies of 10 percent should be possible in a similar device. Baer and Keirstead [62] showed that such a device could be intracavity doubled to the green with good efficiency using $KTiOPO_4$ (KTP). Up to 11 mW output at 532 nm was achieved. More recently, by use of higher power diode laser arrays, up to 370 mW at 1.06 μm was obtained in CW, TEM_{00} operation. The overall electrical to optical efficiency of this device is 9.1 percent [63]. Single-axial mode operation was demonstrated in a diode laser-pumped, monolithic Nd:YAG laser in a nonplanar ring geometry by Kane *et al.* [64]. This unique device is shown in Fig. 8(a). Up to 25 mW at 1.064 μm was obtained with a measurement limited linewidth of less than 3 kHz over a 100 ms measurement time. Fig. 8(b) shows the beat frequency spectrum between two independent oscillators. This source was used as a master oscillator for a solid-state coherent laser radar system [65]. Kozlovsky *et al.* [66] efficiently frequency doubled this source in an external resonator containing $MgO:LiNbO_3$. The single-axial mode operation and good frequency stability allowed locking of the external cavity to the laser frequency. Up to 2 mW at 532 nm was generated for 15 mW input power at 1.06 μm. A single-axial mode source at 1.319 and 1.338 μm in Nd:YAG using a modified version of the nonplanar ring has been demonstrated by Trutna *et al.* [67]. The modified geometry allows good performance with less applied magnetic field. Owyoung and Esherick [68] have shown rapid stress-induced frequency tuning in a diode laser-pumped, longitudinal geometry Nd:YAG rod. Scan rates of up to 1 THz/s over a 1 GHz range have been achieved. By intracavity frequency summing the 1.06 μm radiation of an Nd:YAG laser and its pump radiation in KTP, Risk *et al.* [69] have demonstrated generation of blue coherent radiation. Under infrared dye laser pumping, 1 mW of blue was generated for 275 mW pump power. Using a 200 mW broad area diode laser, output power was limited to 10 μW due to decreased brightness of the pump source.

Allen *et al.* [70] and Smith *et al.* [71] developed linear diode laser arrays and demonstrated a CW diode laser array-pumped Nd:YAG laser in a transverse geometry. Up

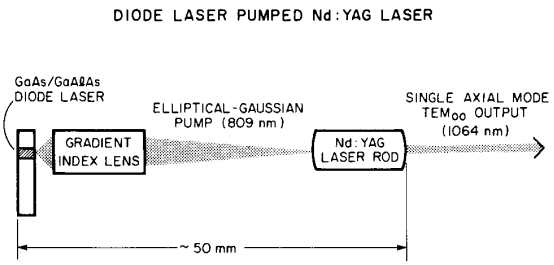

Fig. 7. Schematic of monolithic, diode laser-pumped, longitudinal geometry Nd:YAG laser from [60].

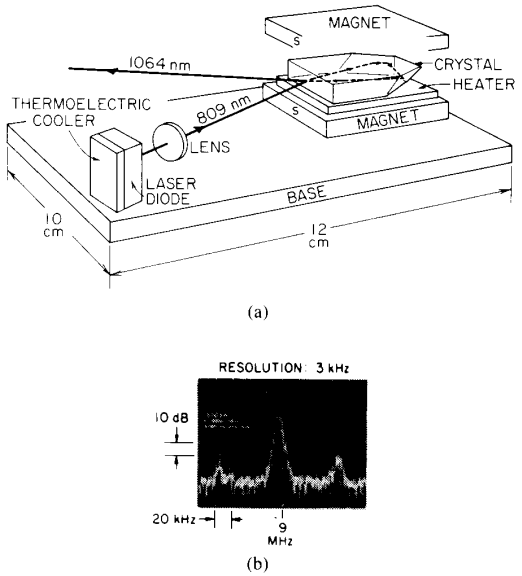

Fig. 8. (a) Schematic of solid-state, unidirectional, nonplanar ring oscillator. (b) Frequency spectrum generated by beating two independent lasers. Linewidth measurement was limited by frequency jitter between the two lasers caused by technical noise.

to 108 mW output at 1.06 μm was achieved for an electrical input to the diode lasers of 25 W. Katzman analyzed the use of a diode laser-pumped Nd:YAG laser for a space communication system [72]. He subsequently demonstrated a diode laser-pumped Nd:YAG as an amplifier for a GaInAsP diode laser [73] which allows direct modulation of the diode to be combined with the higher output provided by the Nd:YAG. Work has continued on using diode laser arrays for side pumping neodymium-doped lasers [74]–[77]. Up to 3 percent overall electrical to optical efficiency has been demonstrated for a CW, TEM_{00} Nd:YAG laser pumped by linear arrays [74]. In a long pulse mode, up to 21 W peak power was obtained from a transverse diode array-pumped Nd:YAG rod at 1.06 μm and up to a 3 W peak power at 532 nm by intracavity SHG with KTP [75]. In a Nd:YAG slab, 170 mJ at 1.06 μm in a long pulse mode has been demonstrated with 6 percent overall electrical to optical efficiency [76]. Reed *et al.* [77] have also demonstrated diode array pumping of Nd:YAG slabs as well as Nd:glass slabs. Up to 70 kW

peak power and 585 mW average power with electrical to optical efficiencies of 4 percent have been obtained.

Advances in Nd-doped fiber devices have also been reported. Diode laser-pumped operation of an Nd-doped SiO_2 single-mode fiber laser as opposed multimode fibers was demonstrated with thresholds under 1 mW for the $^4F_{3/2}$–$^4I_{11/2}$ transition in Nd^{3+} [78]. Much higher gains can be expected in this device compared to the bulk under the same pump power because both the pump and laser beams are guided. Laser action was also reported in a single-mode fiber on the $^4F_{3/2}$–$^4I_{9/2}$ transition in Nd^{3+} near 0.9 μm with low thresholds under R6G dye laser pumping at 590 nm [79]. Diode laser pumping of this transition as well as the $^4F_{3/2}$–$^4I_{13/2}$ transition near 1.4 μm was subsequently reported in a single-mode fiber device [80]. In Nd:YAG fibers, threshold of 4 mW with a slope efficiency of 10 percent was shown in a diode laser-pumped device at 1.06 μm [81].

Neodymium-doped materials other than YAG and stoichiometrics have been used. Other materials have different spectroscopic properties which have advantages over YAG and stoichiometrics. Three important properties are upper state lifetime, absorption spectra, and output wavelength. To obtain larger energy storage, it is desirable to use materials with longer upper state lifetimes. In a pulsed mode, the maximum pulse energy is proportional to the upper state lifetime for a fixed value of CW pump power. The absorption features in the diode laser wavelength band should be wide so that control of the diode laser wavelength is less critical. In addition, it is shown later that the strength of the absorption is a key parameter for these devices. The exact output wavelength of the diode-pumped solid-state laser is important in some applications. For example, the 1.064 μm output of Nd:YAG does not match the peak gain of Nd-doped phosphate glass systems. Fan *et al.* [82] have demonstrated laser operation in Nd:$LiYF_4$ (YLF) which has two times longer upper state lifetime than Nd:YAG and an output wavelength which matches Nd:glass systems. Thresholds were as low as 1 mW and slope efficiencies as high as 38 percent as shown in Fig. 9(a). Intracavity SHG to the green in this device with MgO:$LiNbO_3$ was shown with up to 145 μW single ended output power for 30 mW of pump power. A schematic of this experiment is shown in Fig. 9(b). Kozlovsky *et al.* [83] obtained laser oscillation from Nd:glass in a bulk device. The stimulated emission cross section is lower than Nd:YAG due to inhomogeneous broadening, but glass offers the advantages of a much broader absorption band and lower intrinsic loss. Threshold near 2 mW with slope efficiency of 42 percent was shown under single-stripe diode laser pumping in a longitudinal geometry. Diode-pumped CW operation has also been shown in Nd:MgO:$LiNbO_3$ [84]. This is an interesting laser material because it combines the laser properties of the Nd^{3+} ion with the electrooptical and nonlinear optical properties of the host material. Such a combination allows the construction of devices such as self-frequency-doubled lasers [85] and active internal Q-switched lasers [86] in which the crystal serves as the gain medium and the nonlinear optic or electrooptic crystal simultaneously. The difficulty with $LiNbO_3$ as a host material has been with the photorefractive effect, but the use of diode laser pumping and the addition of MgO allows laser operation with little or no decrease in performance due to the photorefractive effect [84]. Thresholds are near 2 mW with slope efficiencies as high as 39 percent. Fields *et al.* [87] made a comparison of Nd:$La_2Be_2O_5$ (BEL), Nd:YAG, and Nd:YVO_4. They were able to obtain higher slope efficiency and lower threshold for Nd:YVO_4 than for Nd:YAG with 12 percent electrical to optical efficiency. Laser diode pumping of $La_xNd_{1-x}MgAl_{11}O_{19}$ has been demonstrated for helium optical pumping at 1.083 μm in both a longitudinal and transverse pump geometry [88]. The slope efficiency is low, 9.5 percent, compared to other Nd-doped laser and appears to be due to high material loss.

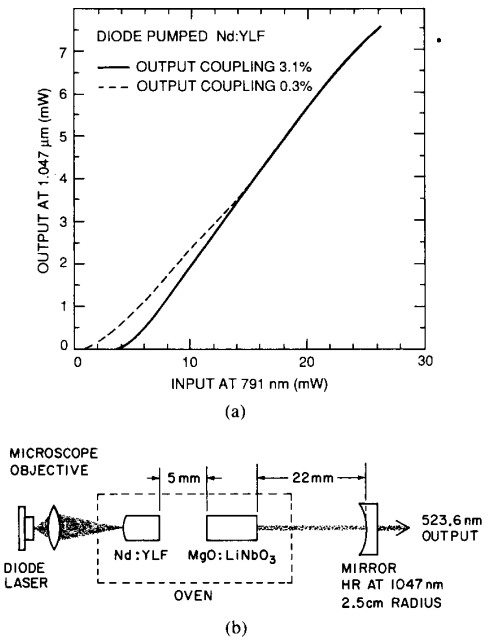

Fig. 9. (a) Output power as a function of incident input power for Nd:YLF with two different values of output coupling. Results are similar to that obtained from Nd:YAG. (b) Schematic of diode laser-pumped, intracavity doubled Nd:YLF laser. The Nd:YLF is ~0.5 cm long and the MgO:$LiNbO_3$ is 0.8 cm long.

There has been progress in operating new transitions under diode pumping. This provides additional wavelengths for these devices and also allows the use of ions which have different spectroscopic properties such as a longer upper state lifetimes. Allen *et al.* [89] demonstrated an end-pumped 2 μm Ho:YAG laser sensitized with Er^{3+} and Tm^{3+} at 77 K on the $^5I_7$–$^5I_8$ transition. Er^{3+} is used to absorb the pump light. This is followed by energy transfer to Tm^{3+} and then to Ho^{3+} to populate the upper laser level. The energy level scheme is similar to that of Castleberry [52] shown in Fig. 6(b), except that the Yb^{3+} is replaced by Er^{3+}. The lower laser level is in

the ground state manifold; thus, the laser is cooled to operate as a four-level laser. A similar device was demonstrated by Hemmati [90] in YLF also with cryogenic cooling. Fan *et al.* [91], [92] have demonstrated single-stripe diode-pumped laser operation on this transition at room temperature in Ho:YAG sensitized with Tm^{3+}. The energy level scheme for this device is shown in Fig. 10(a). The pump radiation is absorbed by Tm^{3+}. This is followed by a cross-relaxation process which allows nearly two excited Tm^{3+} ions to be produced from one absorbed photon. There is rapid energy migration among the Tm^{3+} ions and energy transfer to the Ho^{3+} $^5I_7$ manifold, and laser action is to a level ~ 460 cm^{-1} above the ground state. Threshold of 4.4 mW absorbed pump power with 19 percent slope efficiency were shown. Kintz *et al.* [93] subsequently demonstrated diode laser-pumped operation on this transition as well. Using a 100 mW diode laser array, they obtained over 2 mW output power.

As previously mentioned, laser operation on the $^4F_{3/2}$–$^4I_{9/2}$ Nd^{3+} transition has been demonstrated in fiber devices at room temperature [79], [80]. Fan and Byer predicted by modeling [94] and subsequently demonstrated [94], [95] diode laser-pumped operation of the 946 nm $^4F_{3/2}$–$^4I_{9/2}$ Nd:YAG laser transition at room temperature in a bulk device. The energy level diagram of this quasi-three-level laser is shown in Fig. 1. Threshold of under 10 mW and slope efficiency of 16 percent near threshold were shown. The authors predict slope efficiency of 34 percent for laser operation well above threshold. An all solid-state source in the blue can be obtained by frequency doubling of this device. Intracavity frequency doubling of a 946 nm Nd:YAG laser by $KNbO_3$ has been shown under R6G dye laser pumping with output powers at 473 nm of over 5 mW [96]. Diode array pumping of this transition has also been demonstrated with intracavity frequency doubling by $LiIO_3$ [97]. Output power at 473 nm is limited to 100 μW by the small effective nonlinearity and large Poynting vector walk-off angle of $LiIO_3$ compared to $KNbO_3$.

The 2.3 μm $^3F_4$–$^3H_5$ Tm^{3+} transition as shown in Fig. 10(b) is also of interest. Thomas *et al.* [98] demonstrated laser operation of this transition in Tm:YLF using an alexandrite laser to emulate diode pumping. Operation of this transition was subsequently extended to diode laser pumping [99]. Kintz *et al.* [100] have obtained pulsed and CW laser operation on the 2.8 μm $^4I_{11/2}$–$^4I_{13/2}$ Er^{3+} transition. This laser transition is normally self-terminating, that is, the lower laser level lifetime is longer than the upper laser level lifetime, but CW operation is allowed by a cooperative upconversion process that empties the lower laser level. The energy level scheme is shown in Fig. 11(a). Slope efficiency is limited to 0.7 percent; the authors predict that by optimization of the Er^{3+} concentration and pumping by a single-stripe diode laser, an order of magnitude increase in efficiency is achievable. The Er^{3+} $^4I_{15/2}$–$^4I_{13/2}$ transition near 1.6 μm shown in Fig. 11(b) is of interest for optical communications. Low threshold operation of a fiber laser under dye laser pumping near 800 nm has been demonstrated despite the weak absorption in this wavelength region [101]. More recently, Reekie *et al.* [102] have extended operation to diode pumping with thresholds near 3 mW and output power up to 130 μW.

A number of diode laser-pumped, Q-switched Nd^{3+}-doped lasers have been shown. Up to 150 mJ was obtained from a transverse-pumped Nd:YAG laser with a

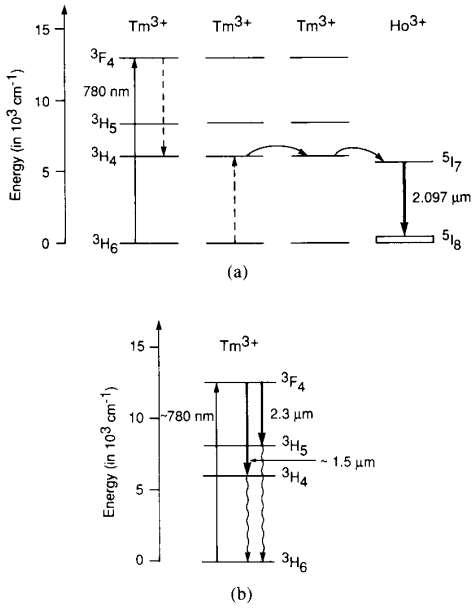

Fig. 10. Energy level schemes in recently demonstrated diode-pumped solid-state lasers. (a) Tm^{3+}, Ho^{3+}:YAG and (b) Tm^{3+}:YAG at 2.3 μm with a possible transition at 1.5 μm also illustrated.

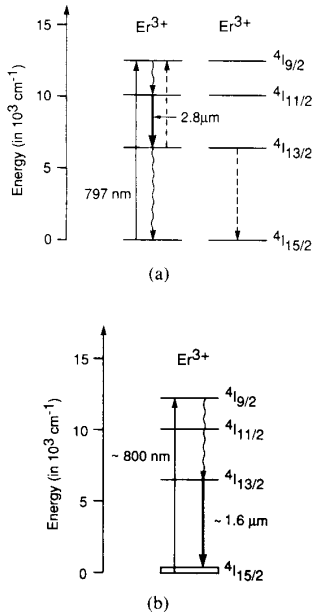

Fig. 11. Energy level schemes in Er^{3+}. (a) $^4I_{11/2}$–$^4I_{13/2}$. (b) $^4I_{13/2}$–$^4I_{15/2}$. Dashed lines in (a) indicate upconversion.

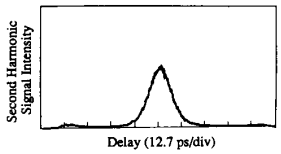

Fig. 12. Autocorrelation trace from a diode laser-pumped, mode-locked, Nd:glass laser.

slope efficiency of 30 percent [103]. In an end-pumped geometry, typical pulse energy obtained from diode array-pumped, Q-switched Nd:YAG lasers is 10 μJ [104]–[106]. By using Nd:YLF, the pulse energy is two times higher for the same pump power [105], [107] as expected. Peak powers in these devices of 2.8 kW for Nd:YLF and 1.2 kW in Nd:YAG have been obtained in 10 ns pulses [107] by pumping with a 200 mW diode laser array. By intracavity frequency doubling a Q-switched Nd:YAG laser with KTP, up to 15 mW average power in the green was generated with 5 μJ per pulse [108]. A miniature end-pumped, mode-locked Nd:YAG laser was developed [109] which could be pumped either by a diode laser or by an R6G dye laser. Pulse widths of 240 ps full width half maximum (FWHM) with pulse energies of 138 pJ were observed. Basu and Byer [110] have shown mode locking in a single-stripe diode laser-pumped Nd:glass and Nd:YAG lasers in a folded three-mirror cavity. Pulsewidths of less than 10 ps FWHM were measured. Fig. 12 shows an autocorrelation trace of the output from this source. Diode laser-pumped Nd:YAG lasers have also been used to injection seed higher power Q-switched Nd:YAG lasers [111]–[114]. One approach has been to use gain-switched diode-pumped rod lasers to produce up to 60 mW of single-axial mode peak power [111]. The output is then injected into the slave laser to force it to run single-axial mode [112], [113]. Injection seeding can also be obtained by using a low-power, ~ 120 μW, CW single-axial mode master oscillator [114].

The field of diode laser-pumped solid-state lasers is moving rapidly. We believe that this historical overview is reasonably complete to the time of writing, although clearly there will be advances in the field before publication of this paper.

III. Comparison of Diode-Pumped Solid-State Lasers to Other Devices

Diode laser-pumped solid-state lasers offer significant advantages over both lamp-pumped solid-state lasers and direct use of diodes. In this section, we compare diode-pumped solid-state lasers to these other devices.

A. Diode-Pumped Versus Lamp-Pumped Solid-State Lasers

Diode-pumped solid-state lasers offer the main advantages of higher efficiency and better frequency stability than lamp-pumped devices. The highest efficiency diode laser-pumped solid-state lasers to our knowledge is that of Fields *et al.* [87] with 12 percent electrical to optical efficiency in Nd:YVO_4 compared to 8 percent in a lamp-pumped Nd:glass laser by Mak *et al.* [115]. The lamp-pumped result was for an atypical pump geometry in which the lamp is located in the center of a hollowed-out cylinder of the gain medium. In the more typical rod geometry, electrical to optical efficiencies on the order of 5 percent have been observed for Nd:Cr:GSGG [116]–[118] and liquid O_2-cooled Er, Tm, Ho:YAG [119]. Thus, diode laser pumping allows on the order of twice the overall efficiency compared to flashlamps at the present time. In the future, the efficiency of diode-pumped solid-state lasers will increase due to increases in diode laser efficiency. The diode laser arrays currently used have typical efficiencies of somewhat greater than 25 percent [120]. However, recent work has shown external quantum efficiencies in diode lasers of 79 percent and overall efficiencies around 50 percent [121] which will lead to increased efficiency for diode laser-pumped solid-state lasers.

The frequency stability and linewidths of diode laser-pumped solid-state lasers is better than that for lamp-pumped lasers due to decreases in technical noise because of the reduced need for cooling and more stable pump sources. Diode-laser pumped solid-state lasers have demonstrated linewidths of 3 kHz measurement limited [64] compared to lamp-pumped linewidths of 120 kHz [122]. The 3 kHz measurement limit is attributed to jitter due to residual pump fluctuations.

Higher average powers can presently be obtained from lamp-pumped systems. However, scaling to higher average powers for diode-pumped systems appears feasible due to rapid advances in diode laser array technology.

B. Diode-Pumped Solid-State Lasers Versus Direct Use of Diodes

Diode laser-pumped solid-state lasers have the advantages of narrower linewidth, higher peak powers, and higher brightness compared to the direct use of diodes. Solid-state lasers have the potential to have narrower linewidths than the measurement limited 3 kHz already demonstrated [64]. The fundamental limit on laser linewidths is given by the Schawlow–Townes equation given by [123]

$$\Delta\nu = h\nu/(2\pi\tau_c{}^2P) \tag{1}$$

where $\Delta\nu$ is the linewidth in hertz, τ_c is the cavity decay time, P is the output power, and $h\nu$ is the output photon energy. The Schawlow–Townes linewidth limit for these devices is less than 1 Hz for 1 mW output [60]. Monolithic diode lasers have much larger linewidth limits than solid-state lasers because of short cavities and low reflectivity of the facets which lead to small τ_c. τ_c for solid-state lasers is on the order of 10^3 larger than for monolithic diode lasers; thus, the fundamental linewidth is 10^{-6} smaller. The linewidth of diode lasers can be reduced by going to external cavity diode lasers, but only at the expense of increased complexity.

Diode-pumped solid-state lasers can have enhanced peak powers because of their long upper state lifetime.

While the peak powers of diode lasers can be enhanced by pulsing, the increase is limited to about an order of magnitude because diode lasers are essentially CW devices. The demonstrated enhancement of peak power from solid-state lasers over the CW power of diode lasers is greater than 10^4 in a Q-switched Nd:YLF laser [107]. Larger increases in peak power may be possible with longer lifetime, higher energy storage materials.

In addition, diode-pumped solid-state lasers can have higher brightness than diode lasers. For example, in an end-pumped geometry, it is easy to convert the output of current diode laser arrays with beams with two lobed output into a TEM_{00} diffraction-limited output from a solid-state laser [61], [63]. In systems with single-stripe diode laser pump beams, the typical elliptical output beam from the diode laser is converted to a round beam; thus, astigmatism is eliminated.

There are also other advantages of diode-pumped solid-state lasers over lamp-pumped devices and direct use of diode lasers which cannot be quantified. For example, diode-pumped solid-state lasers allow simpler design due to reduced need for cooling. In many cases, air cooling is sufficient as opposed to the liquid cooling often required for lamp-pumped systems. Diode-pumped solid-state lasers offer the possibility of operation in wavelength regions where diode lasers either perform poorly or are not available.

It is clear that diode-pumped solid-state lasers offer some significant advantages over lamp-pumped devices and direct use of diodes. However, there are disadvantages as well. Currently, the cost of diode lasers is higher than for the equivalent power flashlamps, but the cost of diode lasers has dropped significantly in the past few years. Projections indicate that the price decrease should continue over the next few years as the sales volume increases. Diode-pumped solid-state lasers are obviously less efficient than the diode lasers themselves and more complex, but these disadvantages must be weighed against the significant advantages in various applications.

IV. Modeling of End-Pumped Lasers

There are a number of reports on the modeling of CW end-pumped Nd^{3+} lasers to derive threshold and slope efficiency. In this section, we summarize the results and derive scaling laws to show the importance of various spectroscopic parameters. A number of workers have developed rate equation models for CW end-pumped four-level Nd^{3+} lasers with the spatial variation of pump and intracavity circulating intensity included [31], [32], [49], [124]–[127]. Casperson [128] has shown the importance of including the spatial variation as opposed to the assumption of uniform pumping and extraction. While the exact formalism between the previous works may be different, the essential results as far as threshold and slope efficiency are the same. Recently, the rate equation models for the four-level lasers have been extended to include the case where there is significant population in the lower laser level in equilibrium, that is, quasi-three-level lasers [94]. The quasi-three-level case is important because a number of potential diode laser-pumped solid-state laser transitions are quasi-three level at room temperature.

There are a number of assumptions used in developing these models about the spectroscopy of the transitions. 1) It is assumed that a constant fraction η_p of the excitations to the pump band relax to the upper laser level. 2) The relative populations of the Stark splittings within a manifold can be given by a Boltzmann distribution at all times. 3) Relaxation from the lower laser level is infinitely fast. 4) Losses are low so that the low gain approximation is valid. 5) The population of the lower laser level in equilibrium is small compared to the doping concentration. 6) The pump band and upper laser level populations at threshold are such that depletion of the ground state population can be ignored. 7) There are no higher order processes such as excited state absorption or cooperative upconversion. These assumptions are realistic for CW Nd^{3+} lasers and for a number of other laser transitions in rare earth ions. For transitions such as the 2.8 μm $^4I_{11/2}$–$^4I_{13/2}$ Er^{3+} transition which is self-terminating [129] or the 2.1 μm Tm, Ho:YAG laser which has energy transfer upconversion [92], these assumptions are not valid and additional terms are required in the rate equations. However, this model still allows insights to be made about these other transitions. For the geometry of the device, we assume negligible diffraction of the pump laser cavity modes in the gain medium, the cavity length is that of the gain medium, and both the pump beam and laser cavity mode are TEM_{00} Gaussian beams. Within the formalism developed later, none of these assumptions is necessary, but they simplify calculations with little affect on the accuracy of the answers.

A. Threshold

A rate equation approach is used to derive the population of the upper laser level which gives the gain of the device. Then the threshold condition that roundtrip gain equals roundtrip loss is used to derive an expression for the threshold power. The upper laser level population N_b at or below threshold is given by

$$\frac{dN_b(r, z)}{dt} = 0 = -\frac{N_b(r, z)}{\tau} + Rf_b r_p(r, z) \qquad (2)$$

where τ is the upper manifold lifetime, f_b is the fraction of the upper manifold population in the upper laser level, and $r_p(r, z)$ is the normalized pump intensity distribution in the gain medium. The first term on the RHS is a relaxation term due to spontaneous emission and nonradiative relaxation and the second term is due to pumping. R is the total pump rate given by

$$R = \eta_p P_a / h\nu_p \qquad (3)$$

where P_a is the absorbed pump power, $h\nu_p$ is the pump photon energy, and η_p is the pump quantum efficiency which is the number of ions in the upper manifold created by one absorbed photon. The roundtrip gain is equal to $2\sigma\Delta N(r, z)L$ where σ is the stimulated emission cross

section, $\Delta N(r, z)$ is the population inversion density, and L is the gain medium length. $\Delta N(r, z)$ is given by $N_b(r, z) - N_a(r, z)$ where $N_a(r, z)$ is the population of the lower laser level. However, the spatial distribution of the pump and laser cavity mode must be taken into account. This can be done by calculating an overlap integral which averages the upper laser level population given by (2) over the laser cavity mode. The threshold condition is then

$$\iiint 2\sigma L s_0(r, z)\left[\eta_p f_b P_{a,\text{th}} r_p(r, z)\tau/h\nu_p - f_a N_0\right] dV = \delta \tag{4}$$

where $s_0(r, z)$ is the normalized cavity mode intensity distribution in the gain medium, $P_{a,\text{th}}$ is the absorbed pump power at threshold, f_a is the fractional occupation of the lower laser level given by a Boltzmann distribution, N_0 is the dopant concentration, and δ is the roundtrip loss. The quantity $f_a N_0$ is equal to N_a, and we have assumed no ground state depletion; thus, N_a does not vary with position at threshold. Equation (4) can be rewritten

$$P_{a,\text{th}} \iiint s_0(r, z)\, r_p(r, z)\, dV = \frac{h\nu_p}{\eta_p \sigma_e \tau L}\left(\frac{\delta_e}{2} + \alpha_i L + \alpha_l L\right). \tag{5}$$

The roundtrip loss δ has been written in terms of $\delta_e + 2\alpha_i L$ where δ_e, the extrinsic loss, is due to losses not dependent on the length of the gain medium such as output coupling, scattering at interfaces, and Fresnel reflections and $\alpha_i L$ represents losses which are proportional to the gain medium length such as impurity absorption and bulk scattering. δ_e can be further written as $T + \delta_f$ where T is the loss due to output coupling and δ_f is the rest of the extrinsic loss. The substitution $\sigma f_a N_0 = \alpha_l$ has been performed where α_l is the absorption coefficent at the laser wavelength in the gain medium due to the lower laser level population. Finally, σ_e, the effective stimulated emission cross section, has been substituted for σf_b. Equation (5) shows that the threshold power is dependent on spectroscopic and material properties ($h\nu_p$, η_p, σ_e, τ, α_l, α_i), and geometry factors through the overlap integral and design choices (L, T). The geometry factors and design choices are not independent of each other nor independent of the spectroscopic properties as discussed later. To carry this calculation further, functional forms must be assumed for $s_0(r, z)$ and $r_p(r, z)$. We assume that the pump and laser cavity modes are TEM_{00} Gaussian beams with negligible diffraction in the gain medium. Then

$$r_p(r, z) = \frac{2\alpha}{\pi w_p^2\left[1 - \exp(-\alpha L)\right]} \exp(-\alpha z) \exp\left(\frac{-2r^2}{w_p^2}\right) \tag{6a}$$

$$s_0(r, z) = \frac{2}{\pi w_0^2 L} \exp\left(\frac{-2r^2}{w_0^2}\right) \tag{6b}$$

where

$$\iiint r_p(r, z)\, dV = \iiint s_0(r, z)\, dV = 1. \tag{6c}$$

α is the absorption coefficient at the pump wavelength, w_p is the Gaussian beam radius of the pump beam, and w_0 is the Gaussian beam radius of the laser cavity mode. The radii are defined such that at $r = w_p$ or $r = w_0$, the electric field amplitude is $1/e$ of that at $r = 0$. It is possible to account for different pump distributions [31], [125], higher order transverse modes [49], [124], noncollinear pump beam and cavity mode [124], or diffraction of the beams within the gain medium [126] by assuming the proper forms for $r_p(r, z)$ and $s_0(r, z)$, but these end-pumped devices typically operate in a TEM_{00} mode, and the threshold is not highly dependent on the exact form for $r_p(r, z)$ as long the power can be described as being within some radius $r = w_p$ [125]. Substituting (6) in (5), the absorbed power at threshold is

$$P_{a,\text{th}} = \frac{\pi h\nu_p}{2\sigma_e \eta_p \tau}(w_0^2 + w_p^2)\left(\frac{\delta_e}{2} + \alpha_i L + \alpha_l L\right). \tag{7}$$

For minimum threshold, it is desirable to have low losses and small spot sizes. There are a number of limiting cases which can be considered to see how the minimum threshold scales with the spectroscopic parameters.

It would be useful to find the scaling of minimum threshold with spectroscopic and material dependences so a figure of merit for threshold can be formulated which allows side-by-side comparison of laser materials. Threshold is inversely proportional to the quantity $\sigma_e \eta_p \tau$; thus, these spectroscopic properties need to be included in a figure of merit. Spectroscopic properties also ultimately determine the minimum value for the geometry factor in (7). Equation (7) gives a nonphysical answer of a minimum threshold of 0 for infinitely tight focusing. To account for diffraction, the average of values of w_0^2 and w_p^2 in the gain medium can instead be used [126]. These minimum average values are proportional to L. The value of L is a design choice, but to absorb a reasonable fraction of the pump radiation, L should be on the order of or greater than $1/\alpha$. On the other hand, if L is too long, the average spot sizes in the crystal increase, as does the absorption at the laser wavelength both of which increase threshold. Consequently, the value of L chosen will be inversely proportional to α.

Consider three limiting cases to determine how the geometry factor scales with spectroscopic properties. In the limit where $\delta_e >> (\alpha_i + \alpha_l)L$, the threshold scales with the geometry factor in (6) as w_0^2. Thus, the minimum $P_{a,\text{th}}$ is inversely proportional to α. This limit applies for four-level lasers in low-loss material with reasonable output coupling like the 1.06 μm Nd^{3+} transition in many hosts. A second limit is $\alpha_i L >> \delta_e + \alpha_l L$. Minimum $P_{a,\text{th}}$ is proportional to $w_0^2 \alpha_i L$, and thus is inversely proportional to α^2/α_i. This limit applies for four-level lasers if the gain medium is of poor optical quality and has high scatter loss

or if the laser is being operated in a high Q regime in which output coupling has been minimized. The third limiting case is $\alpha_l L >> \delta_e + \alpha_i L$. $P_{a,\text{th}}$ is proportional to $w_0^2 \alpha_l L$, and thus is inversely proportional to α^2/α_l. It is important to include the factor of α_l in the denominator of the scale factor because α in the numerator can be increased by increasing N_0, but this also increases α_l. A typical example of this last limiting case is a quasi-three-level laser. Given the spectroscopic quantities on which $P_{a,\text{th}}$ is directly dependent and the spectroscopic quantities on which the geometry is dependent, a figure of merit for minimum threshold is

$$M_t = \sigma_e \eta_p \tau \times \begin{cases} \alpha & \delta_e >> (\alpha_i + \alpha_l)L \\ \alpha^2/\alpha_i & \alpha_i >> \delta_e + \alpha_l L \\ \alpha^2/\alpha_l & \alpha_l >> \delta_e + \alpha_i L \end{cases} \quad (8)$$

where larger M_t leads to smaller $P_{a,\text{th}}$. This allows a direct comparison of various laser materials based on spectroscopic quantities for minimizing threshold. One other spectroscopic quantity that is of practical interest in the design of these devices is the width of the absorption feature for diode pumping $\Delta\lambda_p$. Wider absorption features are desirable because they allow less stringent requirements of diode laser selection and wavelength control. This perhaps could be incorporated into the figure of merit as well by multiplication of M_t by $\Delta\lambda_p$.

M_t was derived for TEM_{00} pump beams, but in practice, the pump beam is often not a Gaussian beam, especially in diode laser array pumping. However, the figure of merits are still valid. For diode laser array pumping, the dimension of the pump beam in the gain medium is larger than the minimum acheivable cavity mode dimension. The reverse is true under TEM_{00} pumping since the wavelength of the cavity mode is longer than the pump beam wavelength. Hall [130] has shown that for a given value of R_0, the optimum value of w_0 is $w_0 \approx R_0$ where πR_0^2 is the approximate area of the pump beam. For a non-Gaussian pump distribution, the average value of R_0^2 scales as least as fast as L, which is the same scaling as before; thus, the derived values of M_t are still valid.

B. Operation Above Threshold

Operation above threshold also can be treated by a rate equation analysis. Above threshold, the rate equations must account for stimulated emission and the circulating intensity in the cavity. The rate equations above threshold in steady state can be written as [94]

$$\frac{d\Delta N(r,z)}{dt} = 0 = (f_b + f_a) R r_p(r,z) - \frac{\Delta N(r,z) - \Delta N^0}{\tau} - \frac{(f_b + f_a) c\sigma \Delta N(r,z)}{n} S s_0(r,z) \quad (9a)$$

$$\frac{dS}{dt} = 0 = \frac{c\sigma}{n} \iiint \Delta N(r,z) \cdot S s_0(r,z)\, dV - \frac{c\delta}{2nL} S. \quad (9b)$$

ΔN^0 is the equilibrium population inversion density, c is the speed of light, n is the index of refraction of the gain medium, and S is the cavity photon number. Equation (9a) describes the population inversion density. This is essentially (2) written more exactly with an additional term describing the simulated emission (the last term on the RHS). Equation (9b) describes the cavity photon number which is proportional to the circulating power and the output power. The first term on the RHS is an increase in photon number due to stimulated emission and the second term is a decrease in photon number due to losses. An assumption in (9) is that only one transverse mode is considered, although extension to more transverse modes is possible [49], [126]. The assumption of one transverse mode is reasonable for end-pumped systems; as long as the pumped volume lies within the volume of the TEM_{00} cavity mode, single transverse mode operation is easily achievable.

Solving (9a) for $\Delta N(r,z)$ and substituting in to (9b), one obtains

$$\frac{1}{2\sigma L}\left(\delta + 2\alpha_l L \iiint \frac{s_0(r,z)\, dV}{1 + \dfrac{(f_b + f_a) c\sigma\tau}{n} S s_0(r,z)}\right) = (f_a + f_b) R\tau \iiint \frac{r_p(r,z)\, s_0(r,z)\, dV}{1 + \dfrac{(f_b + f_a) c\sigma\tau}{n} S s_0(r,z)} \quad (10)$$

where the substitution $-\sigma\Delta N^0 = \alpha_l$ has been made. The LHS of this equation represents the loss terms of (9b) and the RHS the gain terms. There are two components to the loss term. One is the roundtrip loss δ, and the other is the absorption at the laser wavelength due to lower laser level population. In a four-level laser, this second loss term is 0, and (10) reduces to that for a four-level laser as expected.

To get the output power in terms of the input power, S needs to be solved in terms of R. The number of output photons per unit time S_0 and the output power P_0 are given by

$$P_0 = h\nu S_0 = h\nu \frac{TSc}{2nL}. \quad (11)$$

To solve (10), $s_0(r,z)$ and $r_p(r,z)$ are assumed to be TEM_{00} Gaussian beams. While it is possible to analytically solve the integrals in (10) in some cases, the form of the solution does not lead to physical understanding. However, the results can still be easily described.

First consider a four-level laser where $\Delta N^0 = 0$. It has been noted that a condition for good slope efficiency is w_p

$\leq w_0$ [32]. While slope efficiency is the best for the tightest pump focusing, the increase in slope efficiency is small once the above condition is met. In addition, most of this increase in slope efficiency occurs near threshold [127], but in practice, the operating point will be a few times above threshold. The slope efficiency η for a four-level laser which satisfies the condition $w_p \leq w_0$ is given by

$$\eta \approx \eta_p \frac{h\nu}{h\nu_p} \frac{T}{\delta}. \tag{12}$$

For high slope efficiency, one wants high η_p and low $\delta_f + \alpha_i L$. High slope efficiency can still be achieved by increasing T if these other losses are not low, but this is undesirable because it increases threshold.

The quasi-three-level analysis is somewhat more complicated. The best description is that the lower laser level population acts as a saturable loss. This saturable loss term is given by in (10)

$$\delta_s = 2\alpha_l L \iiint \frac{s_0(r, z)\, dV}{1 + \dfrac{(f_b + f_a)\, c\sigma\tau}{n} S s_0(r, z)}$$

$$= \frac{\alpha_l L I_{\text{sat}}}{I} \ln\left(1 + \frac{2I}{I_{\text{sat}}}\right) \tag{13}$$

where the laser cavity mode is assumed to be given by a TEM_{00} Gaussian beam. The saturation intensity I_{sat} is given by

$$I_{\text{sat}} = \frac{h\nu}{(f_b + f_a)\, \sigma\tau}, \tag{14a}$$

and I is the circulating intensity averaged over the Gaussian beam given by

$$I = \frac{Sch\nu}{\pi w_0^2 nL}. \tag{14b}$$

Near threshold, when the circulating intensity is 0, $\delta_s = 2\alpha_l L$. In other words, the loss is equal to the absorption at equilibrium at the laser wavelength due to the lower laser level population. Therefore, near threshold, the slope efficiency is reduced because of the saturable loss since the slope efficiency now goes as $T/(\delta + \delta_s)$. As the circulating intensity increases, δ_s goes to 0, and thus the slope efficiency approaches that of a four-level laser.

The reason that the lower laser level population acts as a saturable loss can be explained. If $w_p < w_0$, then at threshold, $\Delta N(r, z)$ is negative over much of the cavity mode intensity distribution; thus, in these regions, there is absorption at the laser wavelength which can be viewed as a loss at or near threshold. As the circulating intensity increases, the transition saturates due to absorption of the circulating power; thus, $\Delta N(r, z)$ increases toward 0 in the regions where $\Delta N(r, z) < 0$. At very large circulating intensity, the transition is saturated in essentially the entire volume of the laser cavity mode, and the lower laser level population no longer acts as a loss.

Fig. 13 shows the effect of the lower laser level population on laser output. The input pump rate has been put in terms of $F = R/R_{\text{norm}}$ where $R_{\text{norm}} = \pi w_0^2 \delta / 4\eta_p f_b \sigma\tau$ is the pump rate at threshold for a pump beam focused infinitely small. The output is given in terms of $s = S_0/R_{\text{norm}}$, and p is the quantity $(w_0/w_p)^2$. The roundtrip cavity loss is taken to be due solely to output coupling. With this last assumption and other assumptions made about this model, lasers with the same values of the ratio $2\alpha_l L/\delta$ and p have identical curves for s as function of F. In Fig. 13, the dashed curves are for $2\alpha_l L/\delta = 0$ and the solid curve is for $2\alpha_l L/\delta$ equal to 4.4. The effect of δ_s on η_p near threshold is clear as is the saturation of this loss as the laser is operated farther above threshold. For $\delta_e >> \delta_s$, the quasi-three-level laser acts essentially as a four-level laser.

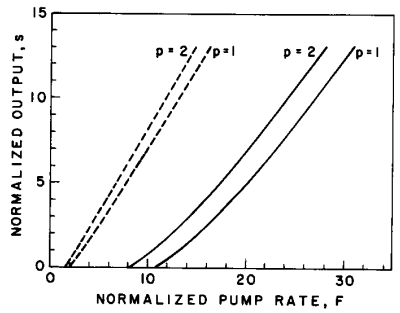

Fig. 13. Normalized output as function of normalized input for quasi-three-level lasers and four-level lasers. The four-level lasers are in the dashed curves. The ratio $2\alpha_l L/\delta$ is 4.4.

A figure of merit M_s can also be formulated for slope efficiency. A reasonable figure of merit for four level transitions is $\eta_p/(\delta_f + 2\alpha_i L)$ since η is directly proportional to η_p and the quantity $\delta_f + 2\alpha_i L$ limits slope efficiency for a given value of T. By making T larger, one can still get good slope efficiency for relatively large values of $\delta_f + 2\alpha_i L$, but only at the expense of increased threshold. We have ignored the quantum defect $h\nu/h\nu_p$ because in comparing two laser materials for a given transition, this quantum defect factor is essentially equal. For quasi-three-level lasers, M_s is dependent on the number of times above threshold. In the limit of far above threshold, the quasi-three-level laser acts as a four-level laser; thus, M_s is the same as above. In the limit of near threshold operation, a better M_s is $\eta_p/(\delta_f + 2\alpha_i L + 2\alpha_l L)$ since this is the quantity which limits η for a given value of T. Thus, M_s can be written as

$$M_s = \begin{cases} \eta_p/(\delta_f + 2\alpha_i L) & \delta_s << \delta_e + 2\alpha_i L \\ \eta_p/(\delta_f + 2\alpha_i L + 2\alpha_l L) & \text{otherwise.} \end{cases} \tag{15}$$

The figure of merits are different for $P_{a,\text{th}}$ and η although they are not contradictory. An overall figure of merit is difficult to derive because it is dependent on operating point. For example, if the laser is operated very far above threshold, M_t is of little consequence. However, these figure of merits still give a basis for comparison be-

tween laser materials based on spectroscopic and material quantities and give some indication of scaling in these devices.

It is often difficult in practice to find the relative figure of merits of various materials since some spectroscopic parameters such as σ can be difficult to measure accurately, while others such as τ and α_p are easy to measure accurately. In addition, not all materials are fully understood. For example, in Nd^{3+} lasers, η_p is often assumed to be 1 based on current understanding of spectroscopy of Nd^{3+}, but this is not verified by slope efficiency measurements. For $\eta_p = 1$, the maximum slope efficiency is given by the ratio of the output photon energy to input photon energy. However, the measured slope efficiencies are consistently below the maximum and are consistent with $\eta_p \approx 0.7$. The discrepancy is not fully understood. Similar difficulties with finding the spectroscopic parameters for other transitions are likely as well, but the figure of merits are still useful in pointing out the key parameters and their importance.

The assumptions used in deriving threshold and slope efficiency accurately describe a number of transitions in solid-state lasers, but transitions such as the 1.6 μm $^4I_{13/2}$–$^4I_{15/2}$ Er^{3+}, Tm-sensitized $^5I_7$–$^5I_8$ Ho^{3+}, and 2.8 μm $^4I_{11/2}$–$^4I_{13/2}$ Er^{3+} do not satisfy the assumptions. The first two transitions have a cooperative energy transfer upconversion process that reduces the upper laser level population below that predicted by (2) [92], [131]. An additional term is needed in (2) to account for the upconversion. This raises the threshold, but has little impact on predicted slope efficiency [131]. Both these transitions are quasi-three level at room temperature. The 2.8 μm Er^{3+} laser is normally self-terminating, but the lower laser level population is reduced by the same cooperative upconversion process that affects the 1.6 μm Er^{3+} laser. Rate equations under uniform pumping for this transition have been treated by Zhekov *et al.* [129] and Pollack *et al.* [132].

It also should be possible to perform a similar analysis for transverse-pumped lasers. However, there are more degrees of freedom in the design of such devices. For example, there are both rod and slab geometry devices, and the output can be extracted in either a single transverse mode or in multiple transverse modes. Thus, the analysis of transverse-pumped devices is more specific to the design of the device than for longitudinal geometry.

V. Wavelength Diversity

Diode-pumped solid-state lasers have been demonstrated on eight transitions in trivalent rare earth ions (RE^{3+}) as well as in Dy^{2+} and U^{3+} at various wavelengths in the near infrared as listed in Table I. It should be possible to operate other transitions in RE^{3+} ions to achieve further wavelength diversity. In this section, we discuss possibilities for new diode laser-pumped transitions in RE^{3+} ions.

The number of possible laser transitions under diode laser pumping is limited by the number of RE^{3+} ions with absorption at diode laser output wavelengths. We limit this discussion to consideration of transitions which can be pumped by GaAlAs diode lasers in the 0.75–0.86 μm wavelength region. RE^{3+} ions with significant absorption in this region are limited to Nd^{3+}, Pm^{3+}, Dy^{3+}, Er^{3+}, and Tm^{3+}. While it should be possible to actually operate a number of the transitions listed below since many have been operated previously to alternative pumping schemes, quantitative modeling is difficult since none of these has been thoroughly characterized spectroscopically.

TABLE I
Diode-Pumped Solid-State Laser Transitions to Date

Ion	Transition	Wavelength (μm)	Temperature (K)
Nd^{3+}	$^4F_{3/2}$–$^4I_{11/2}$	1.06	300
	$^4F_{3/2}$–$^4I_{13/2}$	1.32	300
	$^4F_{3/2}$–$^4I_{9/2}$	0.95	300
U^{3+}	$^4I_{11/2}$–$^4I_{9/2}$	2.61	4.2
Dy^{2+}	$^5I_7$–$^5I_8$	2.36	1.9
Yb^{3+}	$^2F_{7/2}$–$^2F_{5/2}$	1.03	77
Ho^{3+}	$^5I_7$–$^5I_8$	2.10	300
Er^{3+}	$^4I_{11/2}$–$^4I_{13/2}$	2.8	300
	$^4I_{13/2}$–$^4I_{9/2}$	1.6	300
Tm^{3+}	$^3F_4$–$^3H_5$	2.3	300

In Nd^{3+}, one possible transition that has not been demonstrated by diode pumping is $^4F_{3/2}$–$^4I_{15/2}$ at 1.8 μm illustrated in Fig. 1 which Wallace [133] has oscillated by flashlamp pumping. The difficulty is the low cross section compared to that at 1.06 μm (~two orders of magnitude) which will require careful coating design or other form of wavelength selectivity, even in a CW regime. Laser operation should be possible, but because of the low gain compared to 1.06 μm, this transition in unattractive, especially since other transitions also offer promise in this wavelength region.

Pm^{3+} transitions from the $^5F_1$ upper manifold have attractive properties for diode laser pumping [134] as shown in Fig. 14(a). Spectroscopic properties indicate laser operation on the $^5F_1$–$^5I_5$ near 930 nm should operate very similarly to the $^4F_{3/2}$–$^4I_{11/2}$ Nd^{3+} transition. Laser operation was recently demonstrated using this ion [134]. Because Pm is radioactive and is not generally available, it does not appear to be a practical source for most applications.

Dy^{3+} has at least one possible diode laser-pumped transition, $^6H_{13/2}$–$^6H_{15/2}$ near 3 μm as shown in Fig. 14(b). Fig. 14(b) shows direct pumping of Dy^{3+}, but pumping may be possible with a codopant such as Er^{3+} or Tm^{3+} as well. Lamp-pumped laser operation at 77 K was achieved by Johnson and Guggenheim [135] in BaY_2F_8 codoped with Er^{3+}. This quasi-three-level transition at 300 K has a long upper state lifetime, 7 ms, but little else is known spectroscopically. More spectroscopic evaluation of Dy^{3+} is needed before further analysis can be performed on transitions in this ion.

There are additional transitions in Er^{3+} and Tm^{3+} which may be of interest for diode laser pumping. One transition is the Er^{3+} $^4S_{3/2}$–$^4I_{15/2}$ at 550 nm illustrated in Fig. 15(a) by upconversion pumping. Operation of this transition has

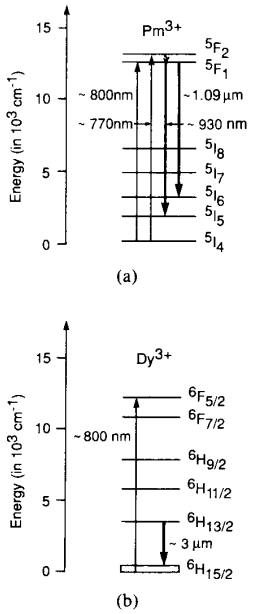

Fig. 14. Possible diode laser-pumped transition. (a) Pm^{3+}. (b) Dy^{3+}.

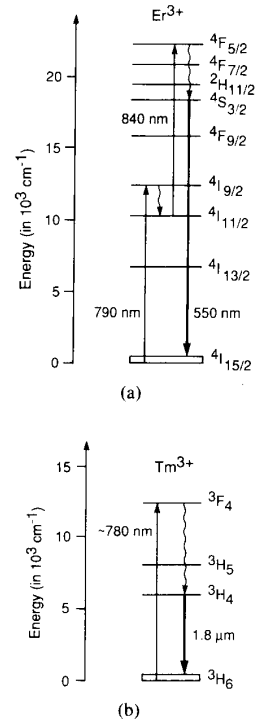

Fig. 15. Possible diode laser-pumped transitions. (a) $^4S_{3/2}$–$^4I_{15/2}$ Er^{3+}. (b) $^3H_4$–$^3H_6$ Tm^{3+}.

been achieved by Silversmith *et al.* [136] by pumping with two IR dye lasers in $YAlO_3$ and by a single IR dye laser in Er:YLF. Cooling to near 77 K is required to reduce the lower laser level population. There are two transitions in Tm^{3+} of interest of diode laser pumping in addition to the already demonstrated 2.3 μm transition. One is the $^3F_4$–$^3H_4$ transition near 1.5 μm shown in Fig. 10(b). Nd^{3+} laser pumped operation has been demonstrated by Antipenko *et al.* [137] in $BaYb_2F_8$:Tm and $LiYbF_4$:Tm. This is a self-terminating transition; thus, laser operation is limited to a pulsed mode, although CW operation may be possible by codoping with another ion to quench the lower laser level. A second possible laser transition is the 1.8 μm $^3H_4$–$^3H_6$ transition shown in Fig. 15(b) which is quasi-three level at room temperature. This transition has a long upper state lifetime which is attractive for high energy storage. By doping heavily enough, a cross-relaxation process would allow pump quantum efficiencies of nearly 2 [138]. We performed an analysis of Tm:YAG which indicated laser operation should be possible with low thresholds at room temperature provided that cooperative energy transfer upconversion effects are negligible.

It is clear that a number of possibilities exist for wavelength extension by operating different transitions in RE^{3+} ions. There may be additional transitions in ions such as RE^{2+}. Many of the possible laser transitions are quasi-three level at room temperature; thus, inclusion of the lower state population in modeling of these lasers is important.

VI. Summary

The field of diode laser-dumped solid-state lasers is moving rapidly. These devices have already been shown to be excellent sources due to their compactness, high efficiency, good frequency stability, and simple design and should find a wide variety of applications. Improvements in these devices are expected. One area for improvement is materials. While Nd:YAG is the laser material of choice for lamp pumping, it may not be optimal for diode pumping. Other Nd-doped materials have longer upper state lifetimes for increased energy storage and peak power in pulsed operation and larger absorption bandwidths for relaxed wavelength tolerance requirements of the diode laser pump sources. For example, laser operation has been demonstrated in $Nd:Na_{0.4}Y_{0.6}F_{2.2}$ [139] which has a lifetime of ~ 800 μs. While other hosts may not have as favorable thermomechanical properties as YAG, this is less important for diode laser pumping because of reduced heating. Scaling to higher powers is also important for many applications. Only end pumping was discussed in depth in this paper, but side pumping is necessary for scaling to higher powers to allow for pumping by arrays of diode lasers. It remains to be seen whether the efficiency of side-pumped devices can approach that of end-pumped devices and do so with near diffraction-limited output beams. One possible approach to pump with arrays in a small volume is to couple the pump power from individual diodes to the gain medium through optical fiber as illustrated in Fig. 16 [140]. Finally, there is interest in new transitions for wavelength diversity. While there are a number of transitions on which laser action can be achieved, ultimately the importance of each transition will depend on a number of factors including overall ef-

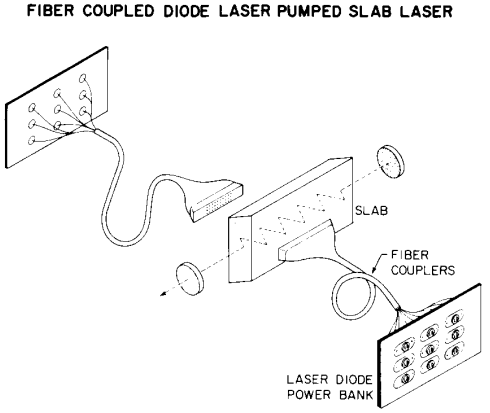

Fig. 16. Schematic of proposed transverse geometry, diode-laser pumped slab laser.

ficiency, ease of operation (for example, is cooling required), energy storage efficiency, and applications in the wavelength band. Spectroscopic measurements of the candidate transitions need to be made to analyze performance. For example, it is important to characterize cooperative energy transfer upconversion in Er^{3+} and the Tm^{3+} sensitized Ho^{3+} laser since this impacts laser threshold and energy storage efficiency. In addition, because of the high pump densities achievable and narrow-band excitation under diode laser pumping, effects which were relatively unimportant in lamp pumping such as excited state absorption at the diode laser wavelength are more crucial.

In conclusion, we have presented a historical overview on diode laser-pumped solid-state lasers. Models for end-pumped devices and figures of merit for these devices were reviewed. Laser transitions which offer the possibility for diode laser pumping are presented. It is clear that diode-pumped solid-state lasers offer the possibility of greatly improved performance over lamp-pumped solid-state lasers and other sources and will be important devices in the future.

References

[1] R. Newman, "Excitation of the Nd^{3+} fluorescence in $CaWO_4$ by recombination radiation in GaAs," *J. Appl. Phys.*, vol. 34, p. 437, 1963.

[2] R. J. Keyes and T. M. Quist, "Injection luminescent pumping of $CaF_2:U^{3+}$ with GaAs diode lasers," *Appl. Phys. Lett.*, vol. 4, pp. 50-52, 1974.

[3] R. N. Hall, G. E. Fenner, J. D. Kingsley, T. J. Soltys, and R. O. Carlson, "Coherent light emission from GaAs junctions," *Phys. Rev. Lett.*, vol. 9, pp. 366-368, 1962.

[4] M. I. Nathan, W. P. Dumke, G. Burns, F. H. Dill, Jr., and G. J. Lasher, "Stimulated emission of radiation from GaAs p-n junction," *Appl. Phys. Lett.*, vol. 1, pp. 62-64, 1962.

[5] N. Holonyak, Jr. and S. F. Bevacqua, "Coherent (visible) light emission from $Ga(As_{1-x}P_x)$ junctions," *Appl. Phys. Lett.*, vol. 1, pp. 82-83, 1962.

[6] T. M. Quist, R. H. Rediker, R. J. Keyes, W. E. Krag, B. Lax, A. L. McWhorter, and H. J. Zeiger, "Semiconductor maser of GaAs," *Appl. Phys. Lett.*, vol. 1, pp. 91-92, 1962.

[7] S. A. Ochs and J. I. Pankove, "Injection-luminescence pumping of a $CaF_2:Dy^{2+}$ laser," *Proc. IEEE*, vol. 52, pp. 713-714, 1964.

[8] M. Ross, "YAG laser operation by semiconductor laser pumping," *Proc. IEEE*, vol. 56, pp. 196-197, 1968.

[9] R. B. Allen and S. J. Scalise, "Continuous operation of a YAlG:Nd laser by injection luminescent pumping," *Appl. Phys. Lett.*, vol. 14, pp. 188-190, 1969.

[10] F. W. Ostermayer, Jr., "$GaAs_{1-x}P_x$ diode pumped YAG:Nd lasers," *Appl. Phys. Lett.*, vol. 18, pp. 93-96, 1971.

[11] F. W. Ostermayer, Jr., R. B. Allen, and E. G. Dierschke, "Room-temperature cw operation of a $GaAs_{1-x}P_x$ diode-pumped YAG:Nd laser," *Appl. Phys. Lett.*, vol. 19, pp. 289-292, 1971.

[12] H. G. Danielmeyer and F. W. Ostermayer, Jr., "Diode-pump-modulated Nd:YAG laser," *J. Appl. Phys.*, vol. 43, pp. 2911-2913, 1972.

[13] N. P. Barnes, "Diode-pumped solid-state lasers," *J. Appl. Phys.*, vol. 44, pp. 230-237, 1972.

[14] L. C. Conant and C. W. Reno, "GaAs laser diode pumped Nd:YAG laser," *Appl. Opt.*, vol. 13, pp. 2457-2458, 1974.

[15] J. E. Jackson and R. R. Rice, "Output fluctuations of high-frequency pulse-pumped Nd:YAG laser," *J. Appl. Phys.*, vol. 45, pp. 2353-1355, 1974.

[16] G. I. Farmer and Y. C. Kiang, "Low-current-density LED-pumped Nd:YAG laser using a solid cylindrical reflector," *J. Appl. Phys.*, vol. 45, pp. 1356-1371, 1974.

[17] Zh. I. Alferov, V. M. Andreev, D. Z. Garbuzov, N. Yu. Davidyuk, V. R. Larionov, P. P. Pashinin, A. M. Prokhorov, V. D. Rumyantsev, V. M. Tuchkevich, and M. M. Khaleev, "YAG:Nd pumping by a planar AlAs-GaAs heterojunction light-emitting diode," *Sov. Phys. Tech. Phys.*, vol. 20, pp. 231-233, 1975.

[18] Zh. I. Alferov, V. I. Bilak, D. Z. Garbuzov, N. Yu. Davidyuk, and M. F. Stel'makh, "Possibility of increasing the pulse power of a $YAG:Nd^{3+}$ laser with semiconductor pump," *Sov. Tech. Phys. Lett.*, vol. 1, pp. 338-339, 1975.

[19] A. L. Zakgeim, Yu. M. Makushenko, V. M. Marakhonov, S. A. Nikishin, and R. P. Seisyan, "Enhanced output of an Nd^{3+}:YAG laser with a semiconductor pump system," *Sov. Tech. Phys. Lett.*, vol. 4, pp. 281-282, 1978.

[20] V. I. Bilak, I. S. Goldobin, G. M. Zverev, I. I. Kuratev, V. A. Pashkov, M. F. Stel'makh, Yu. V. Tsvetkov, and N. M. Solov'eva, "Neodymium YAG laser pumped by light-emitting diodes," *Sov. J. Quantum Electron.*, vol. 11, pp. 1471-1476, 1981.

[21] S. A. Belozerov, L. S. Kornienko, N. V. Kravtsov, I. I. Kuratev, S. I. Rusakov, M. F. Stel'makh, A. A. Shelaev, and A. I. Shelaev, "Nd:YAG solid-state ring laser pumped by a light-emitting diode," *Sov. Tech. Phys. Lett.*, vol. 10, pp. 19-20, 1984.

[22] L. J. Rosenkrantz, "GaAs diode-pumped Nd:YAG laser," *J. Appl. Phys.*, vol. 43, pp 4603-4605, 1973.

[23] R. B. Chesler and D. A. Draegert, "Miniature diode-pumped Nd:YAlG lasers," *Appl. Phys. Lett.*, vol. 23, pp. 235-236, 1973.

[24] D. A. Draegert, "Single-diode end-pumped Nd:YAG laser," *IEEE J. Quantum Electron.*, vol. QE-9, pp. 1146-1149, 1973.

[25] R. B. Chesler and S. Singh, "Performance model for end-pumped miniature Nd:YAlG lasers," *J. Appl. Phys.*, vol. 44, pp. 5441-5443, 1973.

[26] K. Iwamoto, I. Hino, S. Matsumoto, and K. Inoue, "Room temperature cw operated superluminescent diodes for optical pumping of Nd:YAG laser," *Japan. J. Appl. Phys.*, vol. 15, pp. 2191-2194, 1976.

[27] K. Washio, K. Iwamoto, K. Inoue, I. Hino, S. Matsumoto, and F. Saito, "Room-temperature cw operation of an efficient miniaturized Nd:YAG laser end-pumped by a superluminescent diode," *Appl. Phys. Lett.*, vol. 29, pp. 720-722, 1976.

[28] F. W. Ostermayer, Jr., "LED end-pumped Nd:YAG lasers," *IEEE J. Quantum Electon.*, vol. QE-13, pp. 1-6, 1977.

[29] H. P. Weber, T. C. Damen, H. G. Danielmeyer, and B. C. Tofield, "Nd-ultraphosphate laser," *Appl. Phys. Lett.*, vol. 22, pp. 534-536, 1973.

[30] H. P. Weber, "Nd pentaphosphate lasers," *Opt. Quantum Electron.*, vol. 7, pp. 431-442, 1975.

[31] H. G. Danielmeyer, "Stoichiometric laser materials," *Festkörperprobleme XV*, pp. 253-277, 1975.

[32] G. Huber, "Miniature neodymium lasers," in *Current Topics in Materials Science, Vol. 4*, E. Kaldis, Ed. Amsterdam: North-Holland, 1980, pp. 1-43.

[33] S. R. Chinn, J. W. Pierce, and H. Heckscher, "Low-threshold, transversely excited NdP_5O_{14} laser," *IEEE J. Quantum Electron.*, vol. QE-11, pp. 747-754, 1975.

[34] S. R. Chinn, J. W. Pierce, and H. Heckscher, "Low-threshold transversely excited NdP_5O_{14} laser," *Appl. Opt.*, vol. 15, pp. 1444-1449, 1976.

[35] S. R. Chinn, H. Y.-P. Hong, and J. W. Pierce, "Spiking oscillations in diode-pumped NdP_5O_{14} and $NdAl_3(BO_3)_4$ lasers," *IEEE J. Quantum Electron.*, vol. QE-12, pp. 189-193, 1976.

[36] M. Saruwatari and T. Kimura, "LED pumped lithium neodymium tetraphosphate lasers," *IEEE J. Quantum Electron.*, vol. QE-12, pp. 584-591, 1976.

[37] J.-P. Budin, M. Neubauer, and M. Rondot, "Miniature Nd-pentaphosphate laser with bonded mirrors side pumped with low-current-density LED's," *Appl. Phys. Lett.*, vol. 33, pp. 309–311, 1978.
[38] ——, "On the design of neodymium miniature lasers," *IEEE J. Quantum Electron.*, vol. QE-14, pp. 831–839, 1978.
[39] M. Saruwatari, T. Kimura, T. Yamada, and J. Nakano, "LiNd-P_4O_{12} laser pumped with an $Al_xGa_{1-x}As$ electroluminescent diode," *Appl. Phys. Lett.*, vol. 27, pp. 682–684, 1975.
[40] M. Saruwatari, T. Kimura, and K. Otsuka, "Miniaturized cw $LiNdP_4O_{12}$ laser pumped with a semiconductor laser," *Appl. Phys. Lett.*, vol. 29, pp. 291–293, 1976.
[41] K. Kubodera and K. Otsuka, "Efficient $LiNdP_4O_{12}$ lasers pumped with a laser diode," *Appl. Opt.*, vol. 18, pp. 3882–3883, 1979.
[42] G. M. Zverev, I. I. Kuratev, and A. V. Shestakov, "Solid-state microlasers based on crystals with a high concentration of neodymium ions," *Bull. Acad. Sci. USSR Phys. Ser.*, vol. 46, no. 8, pp. 108–112, 1982.
[43] B. I. Denker, A. A. Izyneev, I. I. Kuratev, Yu. V. Tsvetkov, and A. V. Shestakov, "Lasing in phosphate glasses with high neodymium ion concentrations under pumping with light-emitting diodes," *Sov. J. Quantum Electron.*, vol. 10, pp. 1167–1168, 1980.
[44] J. Stone and C. A. Burrus, "Neodymium-doped fiber lasers: Room temperature cw operation with an injection laser pump," *Appl. Opt.*, vol. 13, pp. 1256–1258, 1974.
[45] J. Stone, C. A. Burrus, A. G. Dentai, and B. I. Miller, "Nd:YAG single-crystal fiber laser: room-temperature cw operation using a single LED as an end pump," *Appl. Phys. Lett.*, vol. 29, pp. 37–39, 1976.
[46] C. A. Burrus, J. Stone, and A. G. Dentai, "Room-temperature 1.3 μm c.w. operation of a glass-clad Nd:YAG single-crystal fibre laser end pumped with a single L.E.D.," *Electron. Lett.*, vol. 12, pp. 600–601, 1976.
[47] J. Stone and C. A. Burrus, "Self-contained LED-pumped single-crystal Nd:YAG fiber laser," *Fiber Integrated Opt.*, vol. 2, pp. 19–46, 1979.
[48] K. Kubodera and K. Otsuka, "Diode-pumped miniature solid-state laser: Design considerations," *Appl. Opt.*, vol. 16, pp. 2747–2752, 1977.
[49] ——, "Single-transverse-mode $LiNdP_4O_{12}$ slab waveguide laser," *J. Appl. Phys.*, vol. 50, pp. 653–659, 1979.
[50] ——, "Laser performance of a glass-clad $LiNdP_4O_{12}$ rectangular waveguide," *J. Appl. Phys.*, vol. 50, pp. 6707–6712, 1979.
[51] A. R. Reinberg, L. A. Riseberg, R. M. Brown, R. W. Wacker, and W. C. Holton, "GaAs:Si LED pumped Yb-doped YAG laser," *Appl. Phys. Lett.*, vol. 19, pp. 11–13, 1971.
[52] D. E. Castleberry, "Energy transfer in sensitized rare earth lasers," Ph.D. dissertation, Massachusetts Inst. Technol., Cambridge, 1975.
[53] S. R. Chinn, "Intracavity second-harmonic generation in a Nd pentaphosphate laser," *Appl. Phys. Lett.*, vol. 29, pp. 176–179, 1976.
[54] I. I. Kuratev, "Solid-state lasers with semiconductor pumping," *Bull. Acad. Sci. USSR Phys. Ser.*, vol. 48, no. 8, pp. 104–112, 1984.
[55] K. Kubodera and K. Otsuka, "Spike-mode oscillations in laser-diode pumped $LiNdP_4O_{12}$ lasers," *IEEE J. Quantum Electron.*, vol. QE-17, pp. 1139–1144, 1981.
[56] S. R. Chinn and W. K. Zwicker, "FM mode-locked $Nd_{0.5}La_{0.5}P_5O_{14}$ laser," *Appl. Phys. Lett.*, vol. 34, pp. 847–849, 1979.
[57] K. Otsuka, S. Tarucha, K. Kubodera, and J. Noda, "Gigabit optical pulse generations in integrated lasers, in *Picosecond Lasers and Applications, Proc. SPIE*, vol. 322, 1982, pp. 172–180.
[58] K. Kubodera and J. Noda, "Pure single-mode $LiNdP_4O_{12}$ solid-state laser transmitter for 1.3 μm fiber-optic communications," *Appl. Opt.*, vol. 21, pp. 3466–3469, 1982.
[59] H. R. Telle, "Tunable cw laser oscillation of NdP_5O_{14} at 1.3 μm," *Appl. Phys. B.*, vol. 35, pp. 195–198, 1984.
[60] B. Zhou, T. J. Kane, G. J. Dixon, and R. L. Byer, "Efficient, frequency-stable laser-diode-pumped Nd:YAG laser," *Opt. Lett.*, vol. 10, pp. 62–64, 1985.
[61] D. L. Sipes, "Highly efficient neodymium: yttrium aluminum garnet laser end pumped by a semiconductor laser array," *Appl. Phys. Lett.*, vol. 47, pp. 74–76, 1985.
[62] T. Baer and M. S. Keirstead, "Intracavity frequency doubling of a Nd:YAG laser pumped by a laser diode array," in *Postdeadline Papers, Conf. Lasers Electro-Opt.*, Opt. Soc. Amer., Washington DC, 1985, paper ThZZ1.
[63] J. Berger, D. F. Welch, D. R. Scifries, W. Streifer, and P. S. Cross, "370 mW, 1.06 μm, cw TEM_{00} output from a Nd:YAG laser rod end pumped by a monolithic diode array," in *Postdeadline Papers, Conf. Lasers Electro-Opt.*, Opt. Soc. Amer., Washington, DC, 1987, paper ThT10.
[64] T. J. Kane, A. C. Nielsson, and R. L. Byer, "Frequency stability and offset locking of a laser-diode-pumped Nd:YAG monolithic nonplanar ring oscillator," *Opt. Lett.*, vol. 12, pp. 175–177, 1987.
[65] T. J. Kane, W. J. Kozlovsky, R. L. Byer, and C. E. Byvik, "Coherent laser radar at 1.06 μm using Nd:YAG lasers," *Opt. Lett.*, vol. 12, pp. 239–241, 1987.
[66] W. J. Kozlovsky, C. D. Nabors, and R. L. Byer, "Second harmonic generation of a cw diode-pumped Nd:YAG laser using an externally resonant cavity," *Opt. Lett.*, vol. 13, 1988, to be published.
[67] W. R. Trutna, Jr., D. K. Donald, and M. Nazarathy, "Unidirectional diode-laser-pumped Nd:YAG ring laser with a small magnetic field," *Opt. Lett.*, vol. 12, pp. 248–250, 1987.
[68] A. Owyoung and P. Esherick, "Uses of elastooptically tuned diode laser-excited monolithic (Nd:YAG) lasers," in *Tech. Dig. Conf. Lasers Electro-Opt.*, Opt. Soc. Amer., Washington, DC, 1987, paper WN1.
[69] W. P. Risk, J. C. Baumert, G. C. Bjorklund, F. M. Schellenberg, and W. Lenth, "Generation of blue light by intracavity frequency mixing of the laser and pump radiation of a miniature neodymium: yttrium aluminum garnet lasers," *Appl. Phys. Lett.*, vol. 52, pp. 85–87, 1988.
[70] L. B. Allen, Jr., R. R. Rice, H. G. Koenig, and D. D. Meyer, "Linear array configurations and applications of the double-sided heat sink diode," in *Advances in Laser Engineering and Applications, Proc. SPIE*, vol. 247, 1980, pp. 100–105.
[71] R. J. Smith, R. R. Rice, and L. B. Allen, Jr., "100 mW laser diode pumped Nd:YAG laser," in *Advances in Laser Engineering and Applications, Proc. SPIE*, vol. 247, 1980, pp. 144–148.
[72] M. Katzman, "Laser space communication technology status," in *Control and Communication Technology in Laser Systems, Proc. SPIE*, vol. 295, 1981, pp. 2–9.
[73] M. Katzman, "Lightweight laser transmitter packs power," *Elec. Opt. Syst. Design*, vol. 14, no. 10, p. 12, 1982.
[74] D. L. Begley and D. J. Krebs, "Diode laser-pumped neodymium lasers," *J. Opt. Soc. Amer. A*, vol. 3, no. 13, p. 103, 1986.
[75] F. Hanson, "Laser diode transverse pumping of neodymium laser rods," in *Postdeadline Papers, Conf. Lasers Electro-Opt.*, Opt. Soc. Amer., Washington, DC, 1987, paper ThU3.
[76] R. R. Rice and C. A. Krebs, "Progress in diode pumped lasers," presented at Conf. Lasers Electro-Opt., Baltimore, MD, 1987, paper TuD5.
[77] M. K. Reed, W. J. Kozlovsky, and R. L. Byer, "Diode-laser array pumped neodymium slab oscillators," *Opt. Lett.*, vol. 13, pp. 204–206, 1988.
[78] R. J. Mears, L. Reekie, S. B. Poole and D. N. Payne, "Neodymium-doped silica single-mode fibre lasers," *Electron. Lett.*, vol. 21, pp. 738–740, 1985.
[79] I. P. Alcock, A. I. Ferguson, D. C. Hanna, and A. C. Tropper, "Continuous-wave oscillation of a monomode neodymium-doped fibre laser at 0.9 μm on the $^4F_{3/2} \rightarrow {}^4I_{9/2}$ transition," *Opt. Commun.*, vol. 58, pp. 405–408, 1986.
[80] H. Po, F. Hakimi, R. J. Mansfield R. P. Tumminelli, B. C. McCollum, and E. Snitzer, "Neodymium fiber lasers at 0.905, 1.06, and 1.4 μm," *J. Opt. Soc. Amer. A*, vol. 3, no. 13, p. 103, 1986.
[81] M. J. F. Digonnet, C. J. Gaeta, and H. J. Shaw, "1.064- and 1.32-μm Nd:YAG single crystal fiber lasers," *J. Lightwave Technol.*, vol. LT-4, pp. 454–460, 1986.
[82] T. Y. Fan, G. J. Dixon, and R. L. Byer, "Efficient GaAlAs diode-laser-pumped operation of Nd:YLF at 1.047 μm with intracavity doubling to 523.6 nm," *Opt. Lett.*, vol. 11, pp. 204–206, 1986.
[83] W. J. Kozlovsky, T. Y. Fan, and R. L. Byer, "Diode-pumped continuous-wave Nd:glass laser," *Opt. Lett.*, vol. 11, pp. 788–790, 1986.
[84] A. Cordova-Plaza, T. Y. Fan, M. J. F. Digonnet, R. L. Byer, and H. J. Shaw, "Nd:MgO:$LiNbO_3$ continuous-wave laser pumped by a laser diode," *Opt. Lett.*, vol. 13, pp. 209–211, 1988.
[85] T. Y. Fan, A. Cordova-Plaza, M. J. F. Digonnet, R. L. Byer, and H. J. Shaw, "Nd:MgO:$LiNbO_3$ spectroscopy and laser devices," *J. Opt. Soc. Amer. B*, vol. 3, pp. 140–148, 1987.
[86] A. Cordova-Plaza, M. J. F. Digonnet, and H. J. Shaw, "Miniature CW and active internally Q-switched Nd:MgO:$LiNbO_3$ laser," *IEEE J. Quantum Electron.*, vol. QE-23, pp. 262–266, 1987.
[87] R. A. Fields, M. Birnbaum, C. L. Fincher, "Highly efficient diode-pumped Nd:crystal lasers," in *Tech. Dig., Conf. Lasers Electro-Opt.*, Opt. Soc. Amer., Washington, DC, 1987, paper FL4.
[88] J. Hamel, A. Cassimi, H. Abu-Safia, M. Leduc, and L. D. Schearer, "Diode pumping of LNA lasers for helium optical pumping," *Opt. Commun.*, vol. 63, pp. 114–117, 1987.
[89] R. Allen, L. Esterowitz, L. Goldberg, J. F. Weller, and M. Storm, "Diode-pumped 2 μm holmium laser," *Electron. Lett.*, vol. 22, p.

947, 1986.
[90] H. Hemmati, "Efficient holmium: yttrium lithium fluoride laser longitudinally pumped by a semiconductor laser array," *Appl. Phys. Lett.*, vol. 51, pp. 564-565, 1987.
[91] T. Y. Fan, G. Huber, R. L. Byer, and P. Mitzscherlich, "Continuous wave operation at 2.1 μm of a diode laser pumped, Tm-sensitized Ho: $Y_3Al_5O_{12}$ laser at 300 K," *Opt. Lett.*, vol. 12, pp. 678-680, 1987.
[92] ——, "Spectroscopy and diode laser-pumped operation of Tm, Ho: YAG," *IEEE J. Quantum Electron.*, this issue, pp. 924-933.
[93] G. J. Kintz, L. Esterowitz, and R. Allen, "cw diode-pumped Tm^{3+}, Ho^{3+}: YAG 2.1 μm room-temperature laser," *Electron. Lett.*, vol. 23, p. 616, 1987.
[94] T. Y. Fan and R. L. Byer, "Modeling and CW operation of a quasi-three-level 946 nm Nd: YAG laser," *IEEE J. Quantum Electron.*, vol. QE-23, pp. 605-612, 1987.
[95] ——, "Continuous wave operation of a room temperature, diode laser-pumped 946 nm Nd: YAG laser," *Opt. Lett.*, vol. 12, pp. 809-811, 1987.
[96] G. J. Dixon, Z. M. Zhang, R. S. F. Chang, and N. Djeu, "Efficient blue emission from intensity-doubled 946 nm Nd: YAG laser," *Opt. Lett.*, vol. 13, pp. 137-139, 1988.
[97] W. P. Risk and W. Lenth, "Room temperature, cw 946 nm Nd: YAG laser pumped by laser-diode-arrays and intracavity frequency doubling to 473 nm," *Opt. Lett.*, vol. 12, pp. 993-995, 1987.
[98] M. D. Thomas, H. H. Zenzie, J. C. McCarthy, E. P. Chicklis, and H. P. Jenssen, "Tm^{3+}: YLF laser operation at 2.31 μm," in *Tech. Dig., Conf. Lasers Electro-Opt.*, Opt. Soc. Amer., Washington, DC, 1987, paper THJ4.
[99] G. J. Kintz, L. Esterowitz, and R. Allen, "Cascade laser emission at 2.31 and 2.08 μm from laser diode pumped Tm, Ho: YLF, in *Tech. Dig., Topical Meet. Tunable Solid-State Lasers*, 1987, paper MC2.
[100] G. J. Kintz, R. Allen, and L. Esterowitz, "cw and pulsed 2.8 μm laser emission from diode-pumped Er^{3+}: $LiYF_4$ at room temperature," *Appl. Phys. Lett.*, vol. 50, pp. 1553-1555, 1987.
[101] C. A. Millar, I. D. Miller, B. J. Ainslie, S. P. Craig, and J. R. Armitage, "Low threshold cw operation of an erbium-doped fibre laser pumped at 807 nm wavelength," *Electron. Lett.*, vol. 23, pp. 865-866, 1987.
[102] L. Reekie, I. M. Jauncey, S. B. Poole, and D. N. Payne, "Diode-laser-pumped operation of an Er^{3+} doped single-mode fibre laser," *Electron Lett.*, vol. 23, pp. 1076-1078, 1987.
[103] R. R. Rice, McDonnell Douglas Astronautics Co., St. Louis, MO, private communication.
[104] T. Baer, "Laser diode array pumping of solid-state lasers," in *Tech. Dig. Conf. Lasers Electro-Opt.*, Opt. Soc. Amer., Washington, DC, 1986, paper WG3.
[105] M. Kimball-Linne and T. Baer, "Q-switching of diode-pumped solid-state lasers," in *Tech. Dig. Conf. Lasers Electro-Opt.*, Opt. Soc. Amer., Washington, DC, 1987, paper WS4.
[106] A. I. Ferguson, "Optically pumped Q-switching micro-YAG lasers," in *Tech. Dig. Conf. Lasers Electro-Opt.*, Opt. Soc. Amer., Washington, DC, 1987, paper WS3.
[107] W. Grossman, Lightwave Electronics, Mountain View, CA, private communication.
[108] J. J. Smith and C. Ma, "Power scaling of Q-switched laser-diode-pumped Nd: YAG lasers," in *Tech. Dig. Conf. Lasers Electro-Opt.*, Opt. Soc. Amer., Washington, DC, 1987, paper FL6.
[109] I. P. Alcock and A. I. Ferguson, "Mock-locking and Q-switching of an optically pumped miniature Nd^{3+}: YAG lasers," *Opt. Commun.*, vol. 58, pp. 417-419, 1986.
[110] S. Basu and R. L. Byer, "Diode-laser-pumped mode-locked Nd: glass laser," in *Tech. Dig., Conf. Lasers Electro-Opt.*, Opt. Soc. Amer., Washington, DC, 1987, paper WN3.
[111] A. Owyoung, G. R. Hadley, P. Esherick, R. L. Schmitt, and L. A. Rahn, "Gain switching of a monolithic single-frequency laser-diode-excited Nd: YAG laser," *Opt. Lett.*, vol. 10, pp. 484-486, 1985.
[112] R. L. Schmitt and L. A. Rahn, "Diode-laser-pumped Nd: YAG laser injection seeding system," *Appl. Opt.*, vol. 25, pp. 629-633, 1986.
[113] P. Esherick and A. Owyoung, "Polarization feedback stabilization of an injection-seeded Nd: YAG laser for spectroscopic applications," *J. Opt. Soc. Amer. B*, vol. 4, pp. 41-47, 1987.
[114] M. J. Dyer, W. K. Bischel, and D. G. Scerbak, "Injection locking of Nd: YAG lasers using a diode-pumped cw YAG seed laser," in *Tech. Dig., Conf. Lasers Electro-Opt.*, Opt. Soc. Amer., Washington, DC, 1987, paper WN4.
[115] A. A. Mak, V. A. Fromzel, and A. A. Shcherbakov, "State-of-the-art and prospects for increasing the efficiency of solid-state lasers," *Izv. Akad. Nauk SSSR, Ser. Fiz.*, vol. 48, pp. 1466-1476, 1984.
[116] P. F. Moulton, "Recent advances in solid-state lasers," in *Tech. Dig., Conf. Lasers Electro-Opt.*, Opt. Soc. Amer., Washington, DC, 1984, paper WA2.
[117] E. Reed and E. G. Erickson, "Flashlamp-pumped Q-switched Nd/Cr: GdScGa-garnet laser," in *Tech. Dig., Conf. Lasers Electro-Opt.*, Opt. Soc. Amer., Washington, DC, 1984, paper WA3.
[118] J. A. Caird, W. F. Krupke, M. D. Shinn, L. K. Smith, and R. B. Wilder, Jr., "Measurements of losses and lasing efficiency in Nd: Cr: GSGG laser rods," in *Tech. Dig., Conf. Lasers Electro-Opt.*, Opt. Soc. Amer., Washington, DC, 1985, paper THR3.
[119] R. Beck and K. Gürs, "Ho laser with 50-W output and 6.5% slope efficiency," *J. Appl. Phys.*, vol. 46, pp. 5224-5225, 1975.
[120] P. S. Cross, "Diode array pumps for solid-state lasers," in *Tech. Dig., Conf. Lasers Electro-Opt.*, Opt. Soc. Amer., Washington, DC, 1987, paper WS1.
[121] A. Larsson, M. Mittelstein, Y. Arakawa, and A. Yariv, "High-efficiency broad-area single-quantum-well lasers with narrow single-lobed far-field patterns prepared by molecular beam epitaxy," *Electron. Lett.*, vol. 22, pp. 79-81, 1986.
[122] K. C. Peng, L. A. Wu, and H. J. Kimble, "Frequency-stabilized Nd: YAG laser with high output power," *Appl. Opt.*, vol. 24, pp. 938-940, 1985.
[123] A. L. Schawlow and C. H. Townes, "Infrared and optical masers," *Phys. Rev.*, vol. 112, pp. 1940-1949, 1958.
[124] K. Kubodera, K. Otsuka, and S. Mizazawa, "Stable $LiNdP_4O_{12}$ miniature laser," *Appl. Opt.*, vol. 18, pp. 884-890, 1979.
[125] D. G. Hall, R. J. Smith, and R. R. Rice, "Pump-size effects in Nd: YAG lasers," *Appl. Opt.*, vol. 19, pp. 3041-3043, 1980.
[126] M. J. F. Digonnet and C. J. Gaeta, "Theoretical analysis of optical fiber laser amplifiers and oscillators," *Appl. Opt.*, vol. 24, pp. 333-342, 1985.
[127] P. F. Moulton, "An investigation of the Co: MgF_2 laser system," *IEEE J. Quantum Electron.*, vol. QE-21, pp. 1582-1595, 1985.
[128] L. W. Casperson, "Laser power calculations: sources of error," *Appl. Opt.*, vol. 19, pp. 422-434, 1980.
[129] V. I. Zhekov, V. A. Lobachev, T. M. Murina, and A. M. Prokhorov, "Cooperative phenomena in yttrium erbium aluminum garnet crystals," *Sov. J. Quantum Electron.*, vol. 14, pp. 128-130, 1984.
[130] D. G. Hall, "Optimum mode size criterion for low-gain lasers," *Appl. Opt.*, vol. 20, pp. 1579-1583, 1981.
[131] D. K. Killinger, "Phonon-assisted upconversion in 1.64 μm Er: YAG lasers," in *Tech. Dig., Conf. Lasers Electro-Opt.*, Opt. Soc. Amer., Washington, DC, 1987, paper ThJ4.
[132] S. A. Pollack, D. B. Chang, and N. L. Moise, "Upconversion-pumped infrared erbium laser," *J. Appl. Phys.*, vol. 160, pp. 4077-4086, 1986.
[133] R. W. Wallace, "Oscillation of the 1.833 μ line in Nd^{3+}: YAG," *IEEE J. Quantum Electron.*, vol. QE-7, pp. 203-204, 1971.
[134] M. D. Shinn, W. F. Krupke, T. A. Kirchoff, C. B. Finch, and L. A. Boatner, "Promethium (Pm^{3+}) solid state laser," in *Postdeadline Papers, Conf. Lasers Electro-Opt.*, Opt. Soc. Amer., Washington, DC, 1987, paper ThU17.
[135] L. F. Johnson and H. J. Guggenheim, "Laser emission at 3 μm from Dy^{3+} in BaY_2F_8," *Appl. Phys. Lett.*, vol. 23, pp. 96-98, 1973.
[136] A. J. Silversmith, W. Lenth, and R. M. MacFarlane, "Infrared-pumped erbium laser at 550 nm," in *Tech. Dig., Conf. Lasers Electro-Opt.*, Opt. Soc. Amer., Washington, DC, 1987, paper ThJ2.
[137] B. M. Antipenko, A. A. Mak, O. B. Raba, K. B. Seiranyan, and T. V. Uvarov, "New lasing transition in the Tm^{3+} ion," *Sov. J. Quantum Electron.*, vol. 13, pp. 558-560, 1983.
[138] G. Kintz, R. Allen, and L. Esterowitz, "Two for one photon conversion observed in alexandrite pumped Tm^{3+}, Ho^{3+}: YAG at room temperature," in *Postdeadline Papers, Conf. Lasers Electro-Opt.*, Opt. Soc. Amer., Washington, DC, 1987, paper ThU4.
[139] H. Chou, P. Albers, A. Cassanho, and H. P. Jenssen, "Cw tunable laser emission of Nd^{3+}: $Na_{0.4}Y_{0.6}F_{2.2}$," in *Tunable Solid-State Lasers II*, A. B. Budgor, L. Esterowitz, and L. G. DeShazer, Eds. Berlin: Springer-Verlag, pp. 322-327.
[140] R. L. Byer, "Diode pumped solid-state lasers," *Science*, vol. 239, pp. 742-747, 1988.

T. Y. Fan, for a photograph and biography, see this issue, p. 933.

Robert L. Byer (M'75-SM'83-F'87), for a photograph and biography, see this issue, p. 919.